On-line flatness measurement of large steel plates using moiré topography

Jussi Paakkari

VTT Electronics

V̌TT

TECHNICAL RESEARCH CENTRE OF FINLAND
ESPOO 1998

Dedicated to my wife Outi and daughters Marianna and Tiina

ABSTRACT

The quality demands for steel plate and strip products are increasing, and flatness and dimensional measurements performed on these products must fulfill quality standards, and above all the needs of the clients. Many quality assurance methods exist with regard to flatness and dimensional measurements in the steel industry. Manual gauging methods are often still used, but they are costly in terms of time and labour. Automated non-contact optical measurement systems are becoming more common due to their benefits over traditional methods.

In this thesis a projection moiré topography is applied for automatic measurement of the flatness of large steel plates and a fully automated system applicable to varying surface properties of large steel plates is implemented in a hostile industrial environment. The specifications, design and performance of the system are presented. The measurement area of the system is 3.5 metres x 1.0 metre (width x length), and it achieves a specified depth resolution of 0.3 mm. The system operates in real time on the production line at a speed of 1 m/s.

Experiences gained with the system and the different requirements applying to another measurement site then led to the invention of a novel multipurpose flatness measurement system, the design, laboratory prototype and performance of which are also described in this thesis. The usability and competitiveness of the novel system have been increased by adding 2D dimensional measurements such as edges, widths, lengths etc., and even surface quality inspection, to the same unit. The depth resolution of the laboratory system is better than 0.6 mm.

PREFACE

This thesis is based on the author's research work on moiré topography and 3D machine vision carried out at VTT Electronics during the years 1992 - 1997.

The research and development work was undertaken jointly by following organizations: VTT Electronics, Spectra-Physics VisionTech Oy, Rautaruukki Steel and the Industrial Technology Institute (ITI).

I would like to thank Prof. Matti Pietikäinen of the University of Oulu for his guidance during my studies, and to express special thanks to Dr. Heikki Ailisto and Dr. Ilkka Moring who have both taught me and helped me in the research into 3D machine vision. Ilkka has shown excellent skills in managing and formulating difficult research problems, and we have had many technical discussions with Heikki on new ideas or on problems encountered during the research projects. Thanks also go to Prof. Harri Kopola who has supervised this thesis and improved its standard with his comments and his positive attitude.

I would like to thank my co-workers at VTT Electronics and other research institutes and companies who participated in the flatness measurement projects involving the moiré technique. Particular thanks are expressed to Dr. Kevin Harding and Eric Sieczka for introducing me to the projection moiré technique and fringe images. I must also thank Pekka Kantola, Timo Piironen, Jukka Kinnula and Seppo Lehtikangas for their support and patience during the development of the measurement system. Thanks go to Masa Mäkäräinen and the company CIM-Tech Oy for participating in the development project and making the performance measurements.

Special thanks should be expressed to Professor Henrik Haggrén and Dr. Kevin Harding for the time they have devoted to reviewing and commenting on this thesis. Ms. Tuija Soininen is acknowledged for finalising the drawings, Ms. Irja Kontio for helping with the editing of the text and Mr. Malcolm Hicks for revising the English language.

The Technology Development Centre of Finland (TEKES), VTT, and the above mentioned companies are acknowledged for the support they have given to the research projects on which this dissertation is based. VTT, Tekniikan Edistämissäätiö and Seppo Säynäjäkankaan Tiedesäätiö provided the financial support that enabled me to finish this thesis.

Oulu, April 1998

Jussi Paakkari

CONTENTS

LIST OF SYMBOLS

1D	one-dimensional
2D	two-dimensional
3D	three-dimensional
α	angle between the grid normal and the illumination
β	angle between the grid normal and the observation
ϕ	phase of the moiré signal
δ	noise
σ	standard deviation
a	background intensity of the moiré image
ASTM	American Society for Testing and Materials
b	local contrast value of the moiré image
°C	temperature in degrees Celsius
CAD	computer aided design
CCD	charge coupled device
CMM	co-ordinate measuring machine
d	distance separating the light source and observer
D/A	digital to analog converter
DSP	digital signal processing
EN	European Standard
f	focal length of the projection and observation lenses
G	image intensity
H	height
I	flatness index
l	distance of the light source and observer from the grating plane, when $l_o = l_s$
l_o	distance of the observer from the grating plane
l_p	distance from the reference plane to the centre of the entrance pupils of the projection and observation optics
l_s	distance of the light source from the grating plane
L	wave interval
LCD	liquid crystal display
LP	line pairs
N	contour order
P	image of the projected grating
p	grating pitch
p'	grating pitch of the projected grating onto an object
PLL	phase locked loop
rpm	revolutions per minute
S	steepness index
SCPS	spatial-carrier phase shifting
SFS	Finnish Standards Association
SPS	spatial phase shifting
TDI	time delay and integration
TPS	temporal phase shifting

TTL	transistor-transistor logic
V	virtual binary grating in the computer memory
VTT	Technical Research Centre of Finland
x	Cartesian co-ordinate
y	Cartesian co-ordinate
z	Cartesian co-ordinate
Δz	distance between adjacent contour planes
z_N	contour plane of order N

1 INTRODUCTION

1.1 MOTIVATION

Flatness and dimensional criteria are included in the current quality standards for many sheet and plate products, e.g. steel plates, aluminium plates, door leaves, insulating products for building applications and floor coverings. It is evident that there are many reasons why one would want to know and control the shapes and dimensions of such products. The consumers of steel plate and strip products are increasingly requiring tighter dimensional tolerances and better profiling and shaping. The following motivations for flatness measurement can be listed in the case of steel plates:

❑ Analysis of the flatness of the product assists in process development and diagnostics.

❑ Feedback from flatness measurements to automatic process control using numerical and user-independent information is needed.

❑ There is a need for extremely flat plates for use in automatic welding and plate handling machines.

❑ Plate products need to fulfill quality standards.

❑ Plate products can be classified according to their flatness and prices can be fixed according to this classification.

❑ Mishandling of the plate in lifting, transferring and cutting can locally or totally destroy the flatness of properly processed plates. The steel company can avoid product replacement due to the customer complaints by identifying the plate and recovering its flatness data.

1.2 MEASUREMENT OF THE FLATNESS OF STEEL PLATES

The flatness of a steel plate is specified according to standards to be measured when the plate is lying on a flat surface, the conventional mode of expression being in terms of the maximum deviation from a horizontal flat surface. If the plate under inspection is flat, it will touch the flat surface at every point.

A flatness disturbance can be produced at a hot strip mill by a mismatch between the work roll profile and the incoming strip thickness profile. This will produce a non-uniform reduction across the width of the strip, leading to a non-uniform elongation of the strip in the direction of rolling (Heaven 1988). Other process operations such as cooling, coiling, cutting, lifting and turning can also cause flatness disturbances, which may take several forms.

Common types of disturbances are illustrated in Fig. 1. Attempts may be made to minimize flatness disturbances and internal stresses by means of levelling passes in both hot and cold levelling.

edge waves

side edge waves

center buckle

longitudinal curvature

transverse curvature

waves

folds
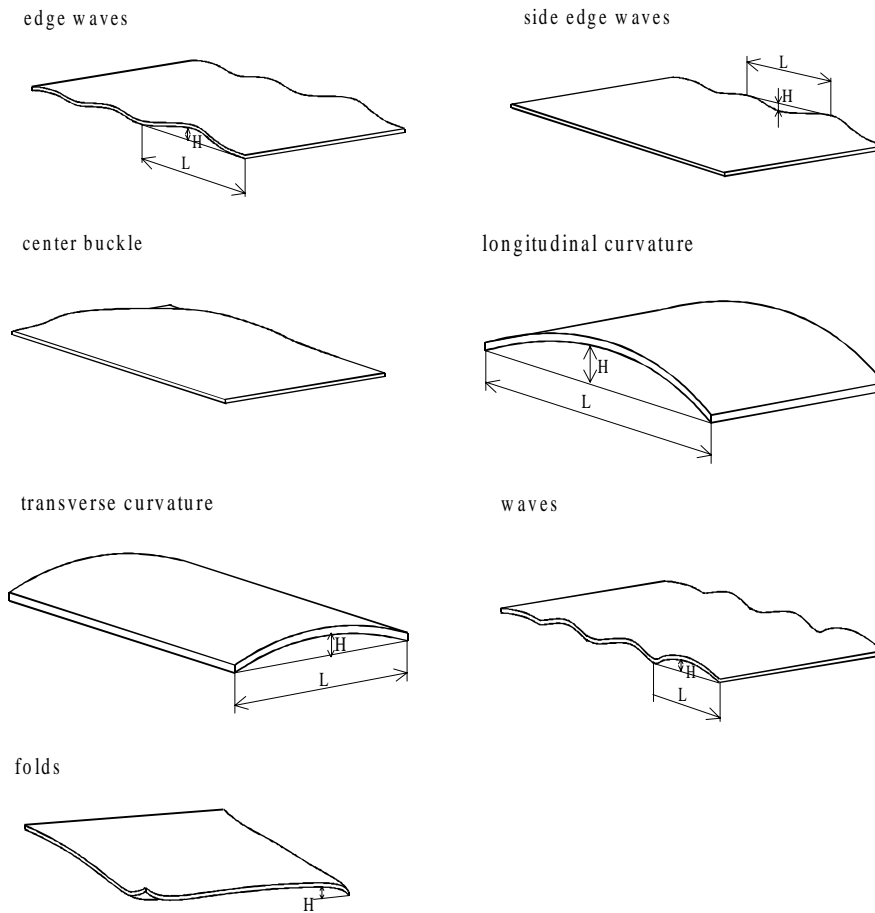
Figure 1. Typical flatness disturbances in steel products.

In addition to the conventional expression of flatness at least two other flatness parameters have been developed and are in use for characterizing sheets with longitudinal waves or buckles (ASTM standard A568/A 568M - 96 1996). These two parameters are a steepness index and a flatness index.

The steepness index is based on a representation of a sheet sample exhibiting edge waves of height H and an interval L, as seen in Fig. 2 a). The height H is typically of the millimetre class. The steepness index value for the sample is defined according to Eq. (1).

$$S = H/L \qquad\qquad (1)$$

The steepness value is often expressed as a percentage:

$$\% \ S = (H/L) \ x \ 100 \ \%. \qquad\qquad (2)$$

Making a series of lengthwise cuts through the sample in Fig. 2 a) relaxes the elastic stresses present in the sheet and results in narrow strips of

12

differing lengths, as shown in Fig. 2 b). Using the length of one of these strips as a reference (L_{ref}), the flatness index, or I-unit value, for an individual strip is defined as:

$$I = (\Delta L/L_{ref}) \times 10^5, \tag{3}$$

where ΔL is the difference between the length of a given strip and the reference strip. For the special case of waves or buckles that are perfectly sinusoidal in character, the following relationship applies between the flatness index (I) and the steepness index (S):

$$I = [(\pi/2)(H/L)]^2 \times 10^5 \tag{4}$$

or

$$I = 24.7S^2. \tag{5}$$

a)

b)

Figure 2.   Representation of a sheet sample with a) edge waves and b) strips of differing length.

There are several general requirements which apply to flatness sensors used in any location to measure flatness at rolling mills (Heaven 1988):

❑ The sensor must not interfere with the process.

❑ The sensor must not damage the surface of the object. It should operate in a non-contact manner.

❑ The sensor must be capable of functioning in a hostile environment. Environmental conditions vary in different parts of the mill.
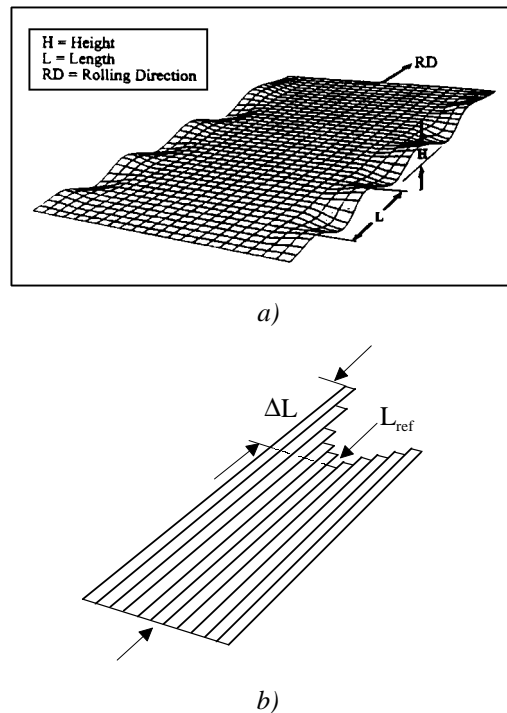
❑ The sensor must be mechanically robust.

❑ The sensor must require minimal maintenance.

❑ Calibration requirements should be minimal.

❑ The sensor should provide accurate, reliable results.

❑ The sensor should sample fast enough and work in real time.

Flatness sensors must meet specific requirements depending on where they are to be used in the mill. In general, sensors should be flexible in design in order to enable modification and customization for different sites. Operator acceptance is always needed in order to extract the full advantage from flatness measurement.

Matsuo et al. (1990) observed that no flatness meters were commercially available that could measure the flatness of steel plates to such a high degree of accuracy as required. To determine the flatness to such close tolerances, plates must be examined with a straight edge by an inspector, i.e. he stops the plate and measures its entire surface with a straight edge, expending much time and labour. In view of the available production capacity, there is a limit to the quality assurance of plates that can be achieved by this inspection method. This paper was written eight years ago, but despite developments in flatness sensors, manual gauging methods are still in common use.

Some steel companies have developed flatness measurement systems of their own. British Steel, for example, has patented a method and apparatus for measuring the shape of the surface of an object (Pat. US. 5,488,478. 1996) in which laser-generated light beams are scanned continuously across the width of the object and an array of linescan cameras are positioned to view and record the light patterns. Scanning is based on an oscillating or rotating mirror. Svenskt Stahl AB has also developed a flatness measurement system in a joint project with the instrument company Selective Electronic Co. AB (Wiese et al. 1982). The system measures the relative length of the material at three or more points across the strip width. Three point triangulation gauges, known as Optogators, are mounted inside a water-cooled air-purged housing about 300 mm above the moving strip.

Flatness measurement methods are nowadays developing rapidly, and several different types of sensors are commercially available. Some examples of commercial flatness measurement systems are presented in Table 1, mostly based on the optical triangulation principle. Triangulation is often implemented using a point laser, laser stripe or grid.

Table 1. Examples of the commercial flatness measurement systems for steel products.

Product	Principle	Measurement area or width	Depth resolution
VSPROF (Rahkola 1997) Vision Systems Oy PL 353 40101 JYVÄSKYLÄ FINLAND	Triangulation based on a laser line and matrix cameras	Width of measurement area 50 to 6500 mm	0.05 mm to 3.0 mm, depending on the measurement area required
ROMETER (Mairy et al. 1988) IRM, Industry Research and Metallurgy Chaussee Churchill, 24 B-4320 MONTEGNEE BELGIUM	Triangulation based on laser points and CCD linescan cameras (five measurement points used as an example)	Width of strip products 500 mm to 2250 mm	0.05 mm (resolution depends on the shape of the triangulation)
LMS Shapemeter (LIMAB 1996) LIMAB Exportgatan 38B, S-422 46 Hisings Backa, SWEDEN	Triangulation based on distance gauges, laser diode as a light source and a 5000 pixel array as a detector	Basic system consists of 10 distance gauges	Not specified
STRESSOMETER roll (ABB 1997) ABB Automation AB S-721 67, Västerås, SWEDEN	Stress distribution measured by a roll with transducers protected by steel rings	The width of the roll can be up to 3300 mm	Smallest stress change to be detected is 0.3 Newton. Normal measurement accuracy is 0.5 I-units.
OptoFlat XAM (Broner Group Ltd. 1991) Broner Group Ltd. P. O. Box 464 Watford WDI 8TS ENGLAND	Structured illumination with phase shifting and CCD camera, reference table	Max. measurement area 62 " x 92" (=1575 mm x 2337 mm), width x length	0.0002" (=0.005 mm)

1.3 CONTRIBUTION OF THIS THESIS

The contribution of this thesis is the development of two flatness measurement systems for steel plates based upon the projection moiré technique. The first employs the traditional technique in which a moiré pattern is formed by projecting a ronchi grating onto the steel plate and comparing this optically with a detection grating. This was the first reported projection moiré system applied in automatic, real time large-scale steel plate flatness measurement at the steel mill. Most projection moiré 3D measurement systems are laboratory prototypes or experimental systems working in supervised and controlled environments, and they tend to measure diffuse objects and are seldom real-time automatic systems. The real-time aspect here does not mean only the capturing of the moiré image and visualization but also fringe interpretation and 3D computation. The following aspects are taken into account simultaneously in the large-scale projection moiré system described in this thesis:

❑ The system can measure large steel plates, maximum area 3.5 metres x 1.0 metre (width x length).

❑ The steel plates to be measured have both diffuse and specular surface properties, which can vary between plate products. The surfaces may also have markings, paintings, dust, water, oil or various kinds of anomalies.

❑ The system operates automatically in real time 24 hours in a day without human intervention. The measurement time required for each image is one second.

❑ A very sensitive projection moiré technique is developed to work in an hostile environment. The system must withstand stray light, dust, vibrations, large electromagnetic fields and ambient temperature variations.

The design and performance of such a system are presented here, and special technical features related to the projection moiré technique that arise from the above considerations are discussed.

The first system was installed at the Rautaruukki Steel mill at Raahe in March 1995, at the end of the mechanical plate cutting line and before the cold leveller, and extended in 1996 to provide fully automatic flatness measurement with a direct connection to the mill's process computer system. The system is now commercially available and is sold by the company Spectra-Physics VisionTech Oy (Spectra-Physics VisionTech 1996).

The author worked as a project manager throughout the development of the measurement system, acting as the chief designer and being personally responsible for the measurement specifications, system integration, the optomechanical set-up and adjustment, the fringe interpretation algorithm

and its implementation, plant installation, the calibration procedure and the performance tests and analysis. He also had an important role in writing the schema and guiding the optomechanical design of the system. He was instrumental in demonstrating that the automatic measurement of the flatness of large steel plates based on projection moiré technology is feasible and operational in a hostile production environment.

Experiences gained from the first pilot installation and the different requirements at other measurement sites guided the invention and development of a second flatness measurement system with the following characteristics:

❑ The system will be installed close to the plate to be measured, and not several metres away. The suitability of close installation depends on the measurement site. The advantages of close-range installation are seeing in production lines with limited space for measuring equipment. No heavy or expensive frame structures are needed.

❑ The system can be easily adapted and scaled for different measurement sites.

❑ The mechanical construction of the system is compact, robust and easy to implement without tight optomechanical tolerances.

❑ The illumination power is better and the contrast of the projected grating is better than in a traditional large-scale projection moiré system.

❑ The system is capable of measuring both diffuse surfaces and fully specular surfaces, as in the case of hot galvanized steel. The effects of surface texture, markings, impurities etc. on the fringe interpretation can be minimized by the use of a background image without projected fringes.

❑ The competitiveness and usability of the flatness measurement system may be improved by building a multipurpose system and adding such measurements as edges, width or surface quality to the same unit.

❑ The moiré signal is robust with respect to stray light on production lines, and if necessary the stray light can easily been blocked out due to the compact optomechanical structure of the system.

The design and performance of the novel multipurpose system are described here and compared with those of the other system. The novel system has been implemented in the laboratory at VTT Electronics, and negotiations are under way for its testing on a production line.

The idea for the novel system was raised by the author, and a patent for the system is pending. The author was the chief designer and did most of the design and implementation work. It was he who demonstrated that the novel multipurpose flatness measurement system is feasible and has advantages over a traditional large-scale projection moiré system.

2 PRINCIPLES AND STATUS OF THE MOIRÉ SHAPE MEASUREMENT TECHNIQUE

The word moiré means a watered or wavy appearance. The term evolved from the ancient French word *mouaire*, which is itself believed to be derived from the English word *mohair*, the wavy fleece of the angora goat. The ancient Chinese developed a technique for pressing two layers of silk together to form wavy patterns on the fabric. European silk and spice traders imported moiré silk and adopted the term into English usage (Pekelsky & van Wijk 1989).

The earliest scientific application of moiré phenomena was described in 1874 by Lord Rayleigh, who suggested testing the quality of replicated diffraction gratings by superimposing a pair of gratings to produce bar patterns, the geometry of which may be analyzed in terms of that of the gratings (Pekelsky & van Wijk 1989).

Moiré topography is used to measure and display the 3D form of an object. The formation of depth contours by arranging the light source and viewing point at the same distance from the grid is a key feature of moiré topography. This concept was formulated independently and concurrently by Meadows et al. (1970) and Takasaki (1970). The shadow and projection methods are the commonly used moiré techniques for 3D shape measurements (Pekelsky & van Wijk 1989).

2.1 MOIRÉ SHAPE MEASUREMENT PRINCIPLES

The main merits of moiré topography are (Patorski & Kujawinska 1993):

❏ Measurements cover a whole field, an advantage over point-by-point methods.

❏ Data acquisition and processing is relatively fast, so that investigations can be carried out in quasi-real time and the process automated.

❏ Profiles are given in the form of 2D contours.

❏ Contouring of specularly reflecting and light scattering surfaces is possible.

❏ The effect of local surface abnormalities may be eliminated by averaging.

❏ The resolution may be varied.

❏ Both differential and absolute measurements are possible.

❏ Both static and dynamic events can be studied.

❏ The method is simple and fast to operate.

2.1.1 Shadow moiré

The shadow method was one of the first scientific applications of moiré techniques. Work in this area goes back to the year 1925 (Mulot 1925), and the method was reintroduced later by a number of authors (Weller & Shephard 1948, Kaczér & Kroupa 1952, Theocaris 1964). All these early authors were concerned with the formation of moiré patterns by a projection of the shadow of a grating on a surface with collimated light and observation of the grating and its shadow so that the viewing point was at infinity (Sciammarella 1982). The arrangement required for this shadow moiré method is based on parallel illumination and parallel reception, see Fig. 3 a). The field equation for the distance Δz between adjacent contour planes can be deduced to be:

$$\Delta z = \frac{p}{\tan(\alpha) + \tan(\beta)},$$ (6)

where α is the angle between the grid normal and the illumination, β is the angle between the grid normal and the observation and p is the grating pitch. The system angle of the moiré instrument is defined as the sum of the angles α and β. The assumption that both the light source and the camera are at infinity limits the method to small models only, of course, as it is difficult to produce collimated light with a large-enough field and the approximation of infinity in the distance between the camera and a large surface is unrealistic.

The illumination and observation conditions were generalized in the 1970's, so that the grating could be illuminated and observed from points at finite distances (Sciammarella 1982). Chiang describes such methods as ones in which the light source and the aperture of the camera lens are approximated by a point but full account is taken of the different angles of illumination and observation (Chiang 1979). It is also assumed that the point light source and the camera lens are located at the same distance from the grating plane. In this case the contours again lie on planes parallel to the grid plane, but the planes are not equally spaced, see Fig. 3 b). The field equation for the contour planes z_N can now be written as:

$$z_N = \frac{Np}{(d - Np)/1},$$ (7)

where N is the contour order, d is the distance separating the light source and the observer and l is their distance from the grating plane. However, if the arrangement is such that $d \gg Np$, and noting that $d/l = \tan(\alpha) + \tan(\beta)$, Eq. (7) can be simplified to:

$$z_N = \frac{Np}{\tan(\alpha) + \tan(\beta)}.$$ (8)

If the point light source and the camera lens are not located at the same distance from the grid plane the contours will not lie on planes but on curved sheets asymptotic to the grid plane, see Fig. 3 c). A field equation has been deduced for this case and is presented by Takasaki (1970) and Meadows et al. (1970), for example.
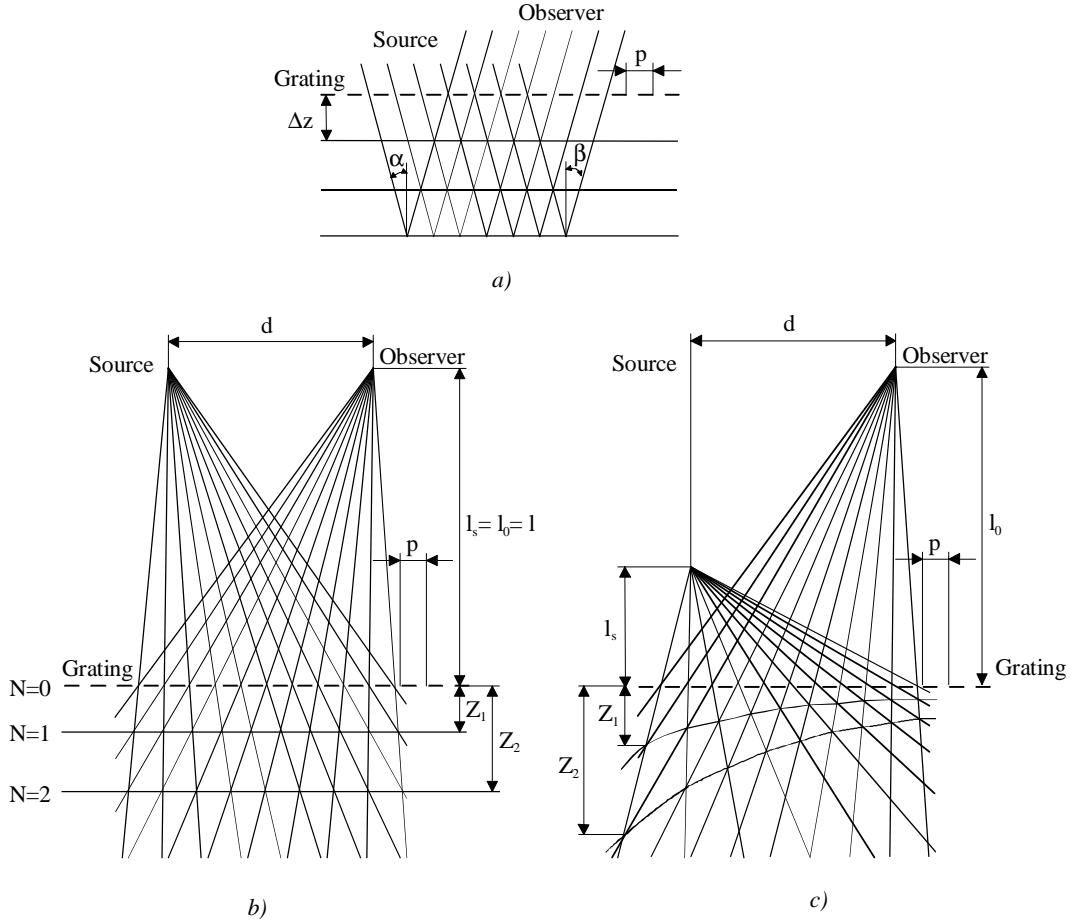
Figure 3. Shadow moiré geometry for a) equal plane contours, b) non-equal plane contours and c) asymptotic curved sheet contours.

2.1.2 Projection moiré

In the projection moiré method the periodic structure is imaged onto the surface to be measured using projection optics. The observation system images the object surface together with the projected periodic structure onto a second periodic structure, called a detection grating, in the image plane. Moiré contours are formed in this plane. The moiré contours have properties analogous to those formed by the shadow moiré technique and the geometrical interpretation of contour formation remains valid. A projection moiré system which generates plane surface contours is presented in Fig. 4. Plane contouring surfaces parallel to the reference plane are obtained if the following conditions are fulfilled:

❏ The projection and detection structures are linear amplitude gratings with binary or sinusoidal transmittance.

❏ The entrance pupils of the optical systems are equidistant from the reference plane.

❏ The optical axes of the projection and observation optics are parallel.

❏ The grating lines are parallel.

❏ The period of the image of the projection grating in the observation plane is equal to the period of the detection grating.
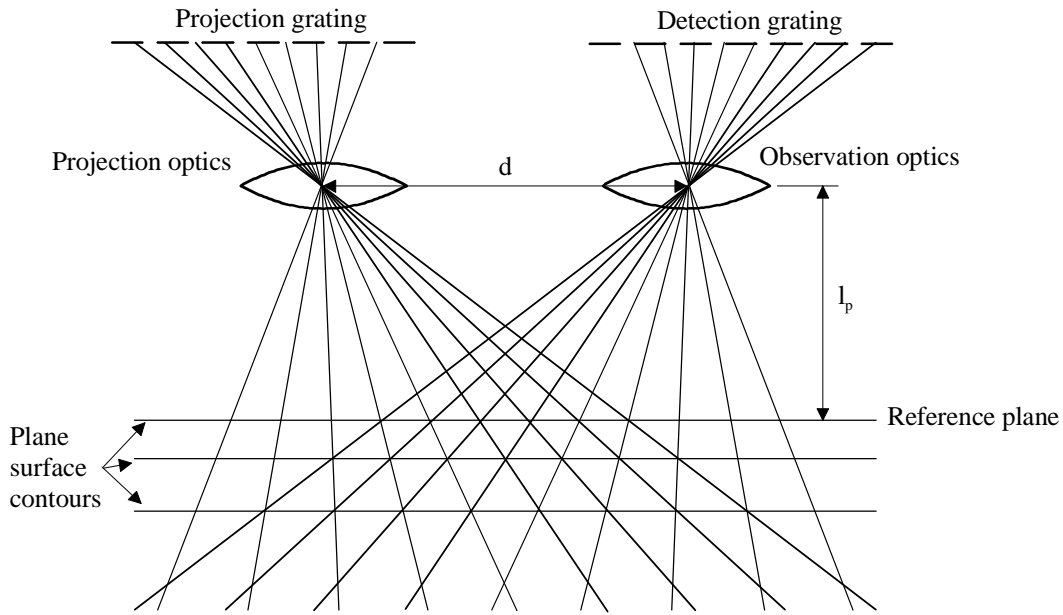
Figure 4.   A projection moiré system which generates plane surface contours.

In the case of projection and observation systems with a parallel axis the elevation of the Nth contour is given by (Takeda 1982):

$$z_N = \frac{Npl_p\,(l_p - f)}{df - Np(l_p - f)},\qquad(9)$$

where p is the pitch of the gratings, l_p is the distance from the reference plane to the centre of the entrance pupils of the projection and observation optics and f is the focal length of the lenses. For practical projection moiré design, the sensitivity per contour interval is approximated by Eq. (10), although one must remember that this assumes the use of collimated light and telecentric observation optics:

$$\Delta z = \frac{p'}{\tan(\alpha) + \tan(\beta)}, \qquad (10)$$

where p' is the grating pitch projected onto the object.

2.2 FRINGE PATTERN ANALYSIS

The output of a topographic shadow or projection moiré system is a contour pattern which must be analysed so that the required 3D information can be formed. The analytical methods applied to interferograms and moiré contours are similar despite the differences in optical principles and image formation. The term fringe is used here instead of contour, because these methods are suitable for many kinds of interferograms and not only for moiré contours. Examples of moiré contour images on a steel plate are presented in Fig. 5.
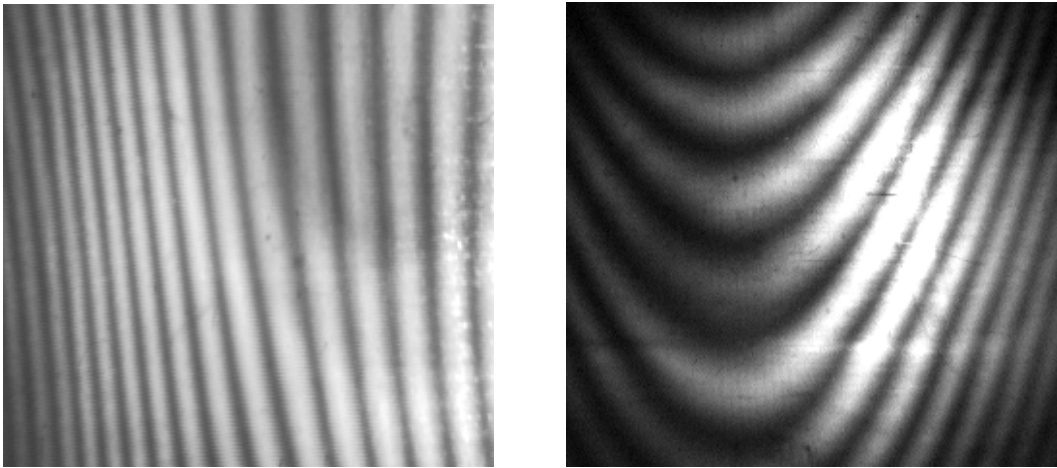
Figure 5. Examples of moiré images.

The measurable quantity in the process of moiré fringe analysis is intensity $G(x, y)$, and the unknown to be extracted is the phase $\phi(x, y)$. The phase information in the fringe pattern is screened by background intensity $a(x, y)$, local contrast $b(x, y)$ and noise δ. The most common expression for the intensity of a moiré fringe pattern is (see Patorski & Kujawinska 1993):

$$G(x, y) = a(x, y) + b(x, y)\cos 2\pi N[\phi(x, y) + \delta)]. \qquad (11)$$

The intensity distribution of a fringe pattern corresponding to Eq. (11) is presented in Fig. 6.
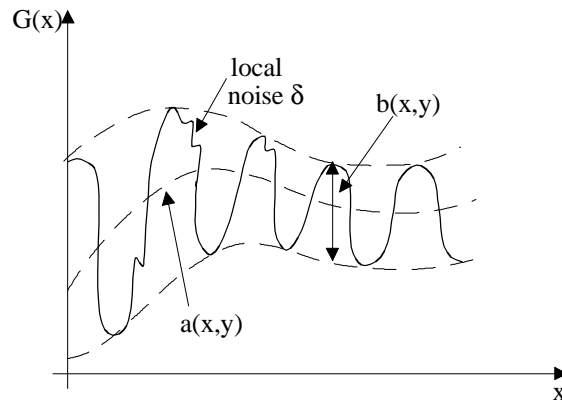
Figure 6. Intensity distribution of a fringe pattern.

The main techniques of automatic fringe pattern analysis employed in moiré topography are presented in Fig. 7.
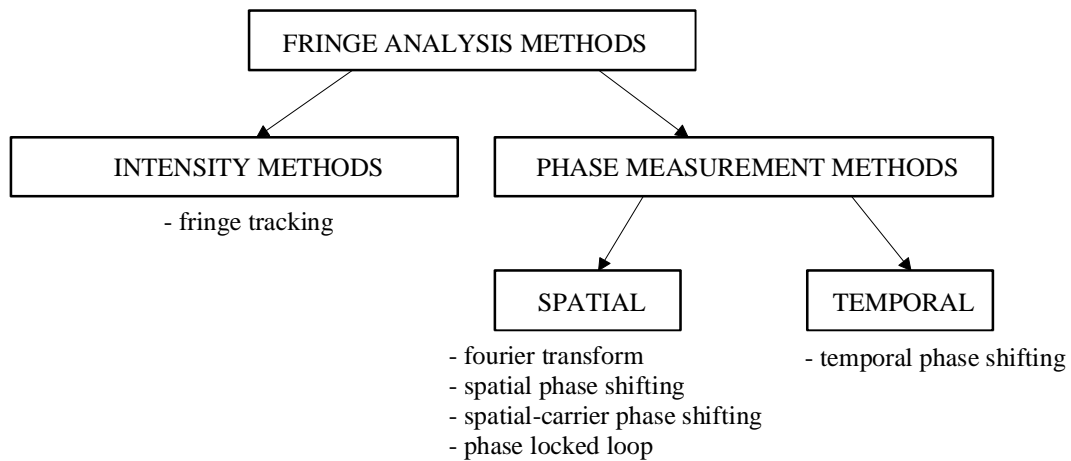
Figure 7. Main fringe pattern analysis techniques used in moiré topography.

Fringe analysis based on intensity information consists of several steps (Patorski & Kujawinska 1993):

1. Acquire and digitize data.

2. Specify the object to be analyzed.

3. Preprocess or enhance the image to reduce the noise.

4. Fringe recognition.

5. Fringe order assignment.

When an intensity method is used the phase is obtained by direct measurement of the intensity variation across the field of view. It is possible to evaluate the phase modulation with one image only. Use of the fringe

tracing method provides a sensitivity of $\pi/20$ (Kozlowski & Serra 1997). These methods are basically fringe following techniques which trace the minimum or maximum level or zero-crossings of the sinusoidal pattern. A summary of the intensity methods is given in Fig. 8.
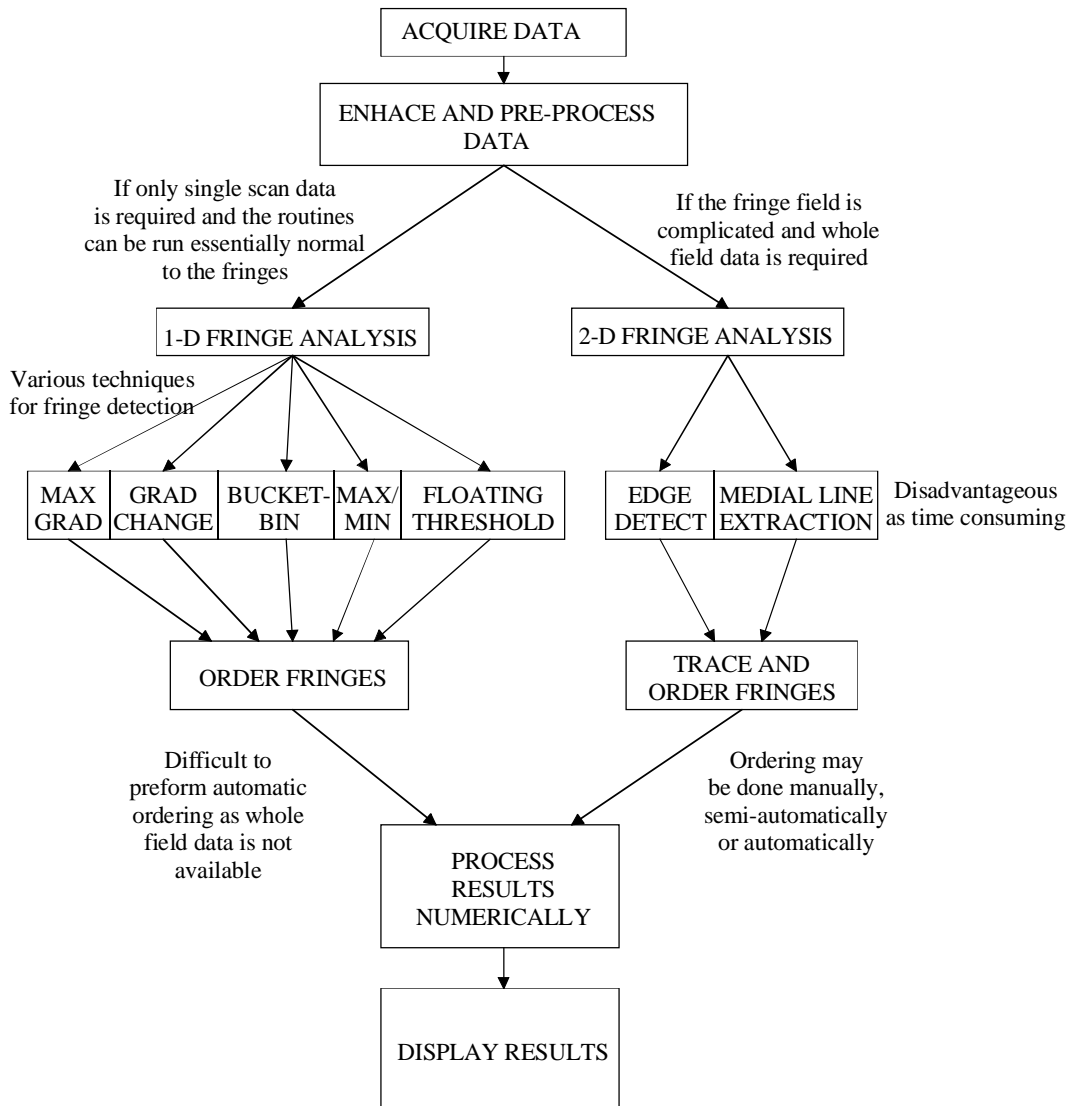
Figure 8. Summary of the intensity methods (Patorski & Kujawinska 1993).

Intensity methods are characterized as achieving low accuracy and being difficult to automate or compute in real time (Kujawinska 1993).

Modern interferogram analysis is based on phase shifting techniques. The phase shift may be introduced between a temporal sequence of interferograms, by splitting and phase shifting the beams in parallel or by introducing a spatial carrier frequency. Phase shifting techniques may be of the temporal (TPS), spatial (SPS) and spatial-carrier (SCPS) types. If a series of images with phase shift is to be analyzed, at least three images are needed. An example of three phase shifted images can be seen in Fig. 9.

The phase information in this simplest case can be expressed according to Eq. (12) (see Schmit 1996)

$$\phi(x,y) = \arctan\left[\frac{G_3(x,y) - G_2(x,y)}{G_1(x,y) - G_2(x,y)}\right]. \qquad (12)$$

Eq. (12) assumes a 90° phase shift between pixels, but algorithms exist which calculate phase information with different phase offsets and numbers of images.

Phase measurement methods of fringe pattern analysis predominate over intensity-based methods in research and in commercially available systems. Most methods tend to be optimized for a particular type of fringe pattern and to give a solution for a particular application (Kujawinska 1993).

According to Kujawinska, each phase measuring method in a fringe pattern includes four general stages:

1. Photoelectric detection of the fringe pattern.

2. Calculation of the phase modulus 2π.

3. Solutions for the modulus 2π and the sign problem.

4. Scaling of the results for various interferometric and moiré techniques and calculation of the relevant physical quantities.

Kujawinska (1993) also gives a schematic representation of a multipurpose system for automatic fringe pattern analysis, which relies on two basic methods: Fourier transform and phase shifting. This representation can be seen in Fig. 9.

OBJECT

MONITOR

| OPTICAL SYSTEM | CCD CAMERA | | D/A CONVERTER | COMPUTER | RGB |

PHASE-MEASURING METHODS

2-D FOURIER

PHASE-SHIFTING

| Temporal | Spatial | Spatial-Carrier |

$FT[I(x,y)]$

I_1 $\quad$ I_2 $\quad$ I_3
δ_1 $\quad$ δ_2 $\quad$ δ_3

$C(f_x - f_0)$

f_x

$\Phi = \arctan \dfrac{\sum I_i \sin\delta_i}{\sum I_i \cos\delta_i}$

$\Phi' = \arctan \dfrac{\sum I_i \sin\delta_i}{\sum I_i \cos\delta_i}$

$FT^{-1}[c(f_x - f_0)]$

$\Phi = \arctan \dfrac{\text{Im}\, c(x,y)}{\text{Re}\, c(x,y)}$

$\Phi = \Phi' - i\pi/2$

| Phase fringes, phase modulo 2π |

| Phase unwrapping, $\Phi(x,y)$ |

| Phase scaling |
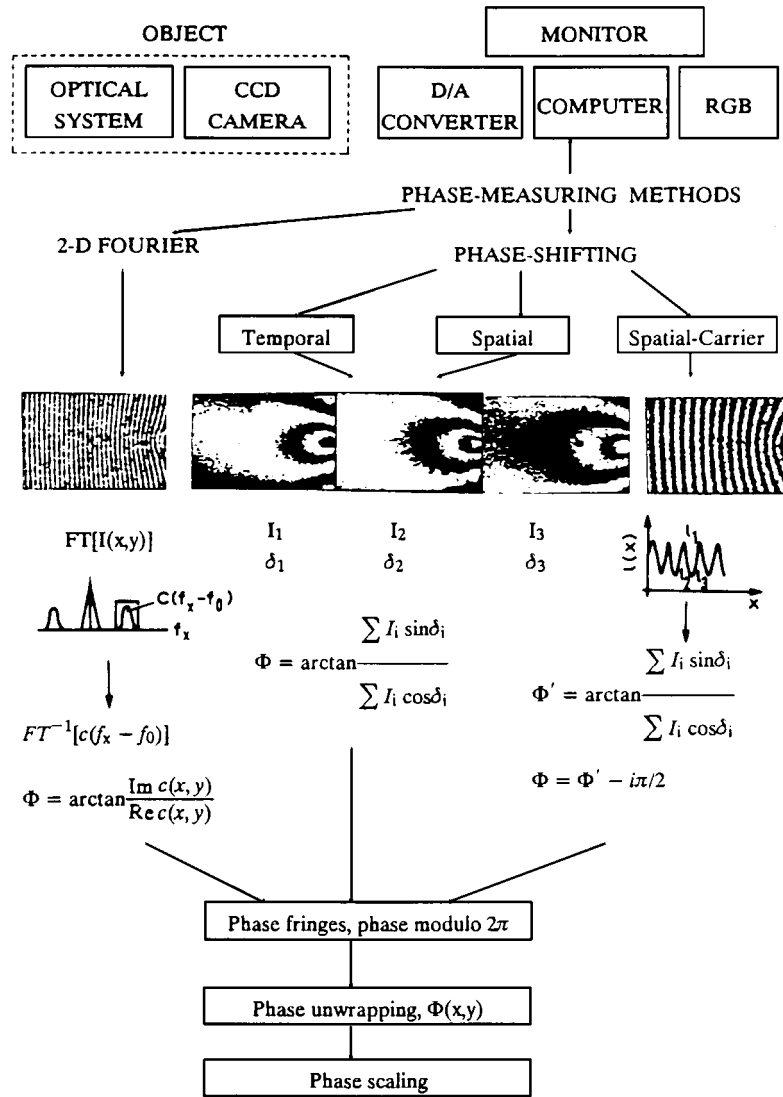
Figure 9. Schematic representation of a multipurpose system for automatic fringe pattern analysis (Kujawinska 1993).

A Fourier transform method (see Fig. 9) is a global operation based on retrieving the phase function in the spatial frequency plane. Only one image is needed. The representation of the 2D fringe pattern for a Fourier method with a spatial carrier is described according to Eq. (13) (Perry & McKelvie 1993).

$$G(x, y) = a(x, y) + b(x, y) \cos[2\pi(f_x x + f_y y) + \phi(x, y)], \qquad (13)$$

where f_x and f_y are the linear carrier components and $\phi(x, y)$ is the phase information of interest. According to Perry & McKelvie (1993), the Fourier method runs into grave difficulties with edge effects and spectral leakage. Spectral leakage means that the Fourier transform will distribute large amounts of energy over a wide range of frequencies due to edges and discontinuities. This not only obscures the signal power, but also makes isolation of a pure signal difficult. This leakage is analyzed in more detail

by Schmit (1996). Discontinuous fringe patterns arise in many practical circumstances and are complicated to analyze. The experience of Perry and McKelvie was that the Fourier method is not capable of providing satisfactory measurements near boundaries and discontinuities, and a further difficulty arises when the signal is not confined to a narrow band of frequencies. This means that a carefully designed filter is required.

The temporal phase shifting technique (TPS), which analyzes three or more interferograms acquired serially over time, forms the basis for most modern interferometers. TPS produces the highest spatial resolution and highest accuracy in the case of static wave fronts, so that unless some good reason exists to use an alternative analysis technique, it is this that will give the best results. TPS is not appropriate in situations where dynamic wave fronts exist, however, or where a phase shifter is not available or quantitative results are not needed (Sough 1993). A digital fringe pattern analyzer for optical metrology has been developed by the Warsaw University of Technology. This uses 3 - 5 phase-shifted images and achieves an accuracy of 1/100 of a fringe (Warsaw University of Technology).

The SPS method analyzes three or more phase shifted interferograms acquired simultaneously. A separate camera and frame grabber must be used for each channel, and the optical paths have to be separated, which needs careful design, alignment of the components and calibration. This may also increase the noise due to the different properties of the separate channels (Sough 1993).

The main requirement in the SCPS technique, introduced in the 1990's, is defining the proper carrier frequency. The SCPS technique is a spatial version of the temporal phase shifting technique (TPS) and the same algorithms can be used in both techniques. The difference is that the temporal technique requires at least three images with 90° phase shift while SCPS needs one image with 90° phase shift from pixel to pixel, equivalent to 4 pixels per fringe. The carrier wave may be introduced by tilting a mirror in an interferometric system or tilting a plane object or rotating the projection or detection grating in a moiré topography.

The SCPS technique is robust and works even when the fringes are of very poor quality. The SCPS technique does not require a phase shifter, but the greatest matter for concern is the anticipated loss in resolution due to spatial variations in either phase or intensity. Discontinuities will introduce global noise into the Fourier transform method, whereas they will lead to localized errors in the SCPS technique, which is based on the sequential pixel processing (Sough 1993).

A problem common to all phase shifting techniques is the unwrapping phase. Obscurations, noise, steep wave fronts or speckle may cause the unwrapping algorithm to fail, and when an error occurs it will propagate from bad pixels to the adjacent pixels.

In addition to intensity, Fourier and phase shifting techniques there exist other methods of fringe pattern analysis. One solution is an application of backpropagation neural networks. This is robust and easy to implement but has the drawback of needing a long training phase. Also, the fringe data need to be preprocessed before training, including the creation of input and output vectors, transformation of the data into a relevant form and the choosing of non-overlapping sub-sets of data for training and testing. The results of both simulated and practical experiments indicate that neural networks can be applied to the analysis of fringe patterns when the application is a matter of classification rather than interpolation (Mills et al. 1995).

A phase-locked loop (PLL) technique has been developed recently for demodulating 2D carrier-frequency fringe patterns. PLL is a spatial technique, the main feature of which is fast phase detection. Also, the unwrapping process is implicit within the phase tracking loop. An extension to the basic PLL scheme has been presented for demodulating noisy fringe patterns, in which the phase in the fringe pattern is estimated iteratively at the same time as the bandwidth of the iterative PLL system is gradually reduced to improve the signal-to-noise ratio of the detected phase and resolve any noise-generated phase inconsistencies. The iterative process requires more computing time, however (Servin et al. 1995).

2.3 CURRENT STATUS OF THE MOIRÉ SHAPE MEASUREMENT TECHNIQUE

The wide availability of digital image processing systems achieved in the 1980's influenced the development of a great number of fringe pattern analysis methods (Kujawinska & Patorski 1993). Gåsvik reported the moiré technique to be a promising method for 3D machine vision in 1989, partly on account of the increasing capacity and decreasing prices of digital image processing plug-in modules for personal computers (Gåsvik et al. 1989). Likewise, Suzuki and Kanaya (1988) that there were prospects that moiré topography would emerge as a more important measurement method and strengthen its position in the near future.

Cardenas-Garcia et al. (1994) state that though many reports have been written on the use of the projection moiré technique, whether automated or not, it is uncommon to obtain detailed specifications on experimental data as to the errors associated with the experimental set-up used. The authors conclude that projection moiré is not an ideal optical technique for making topographical measurements of surfaces. The principal problems related to its implementation in an automated mode are: (1) the ability to make an automatic distinction between a depression and an elevation from a contour map of the object; (2) the assignment of fringe orders automatically, including those separated by discontinuities; (3) the location of the centre lines of broad fringes by correcting unwanted irradiance variations caused by non-uniform light reflection on the object surface; (4) interpolation in

regions lying between contour lines, and (5) evaluation of the existence of false or partially dark fringes. Based on this research projection moiré is characterized as an experimental technique.

It was noted in a US patent issued in 1994 that previous moiré interferometry systems had not been adapted for large panel inspection, but rather were best suited for performing range measurements on small areas. As a result, current moiré interferometry systems are not large enough to analyze large panel surfaces (Pat. US. 5,307,152. 1994). Research into the measurement of large steel plates using projection moiré topography was started at VTT Electronics in 1992. The aim was to demonstrate the feasibility of projection moiré for the automatic flatness measurements performed on large steel plates.

2.3.1 Status of optical moiré shape measurement

This section describes systems employing moiré topography for practical measurements and reviews the technical solutions, design procedures, basic phenomena, device implementations and performance figures. Many phenomena, problems and solutions associated with optical techniques can be associated with other types of implementations of moiré topography as well.

Conventional optical solutions

Conventional optical solutions for shadow and projection moiré implementations are shown in Fig. 10.
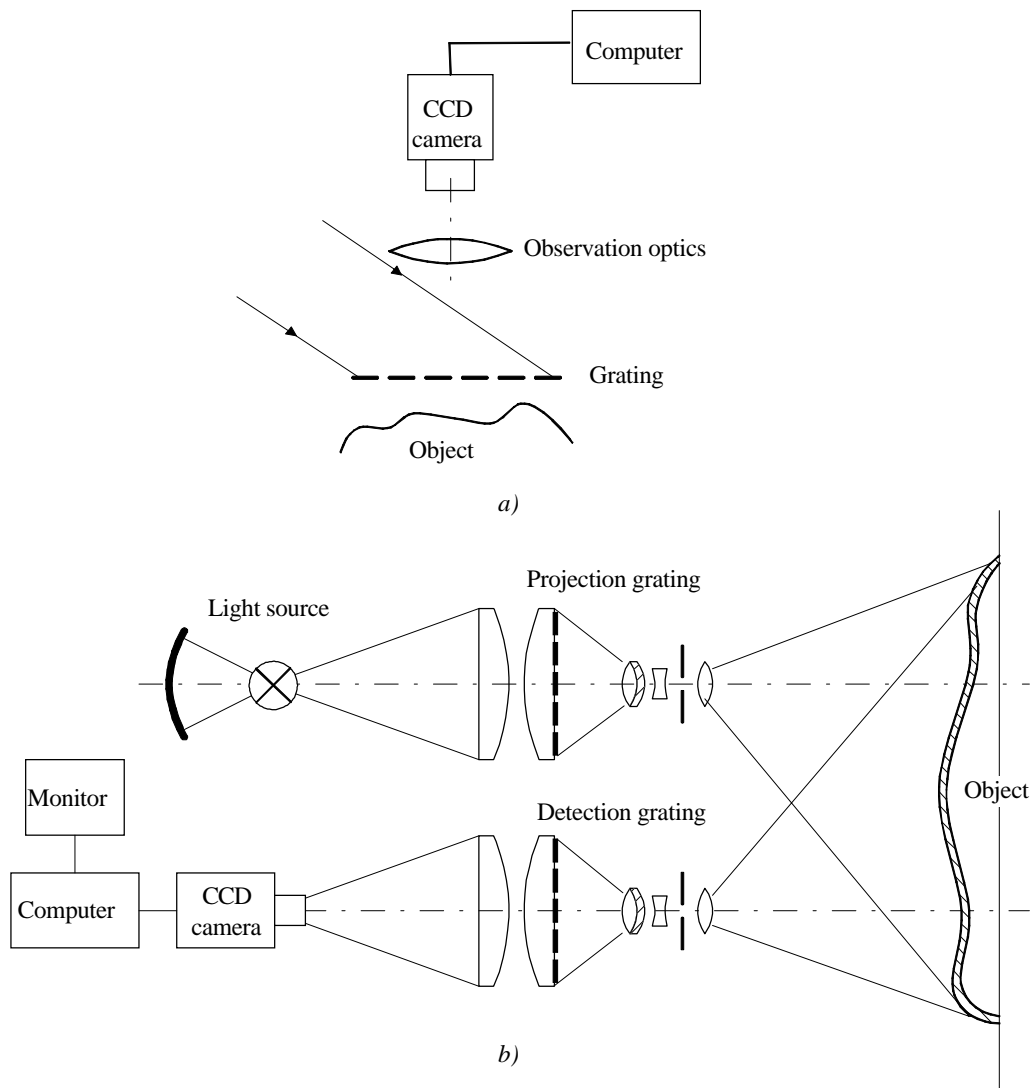
Figure 10. Conventional optical solutions for a) shadow and b) projection moiré instruments.

In the case of the shadow moiré technique one grid is used in combination with a light source and recording equipment, usually a CCD camera (see Fig. 10 a). The grid needs to be installed close to the object to be measured and should be at least as large as the object. The need for a large grid and the limitations on height variations in the object due to the proximity of the grid are sometimes treated as disadvantages of the shadow moiré technique. The contrast of shadow moiré contours is greatly influenced by the size and orientation of the light source.

The optical projection moiré technique is implemented using physical gratings in both the projection and observation systems (see Fig. 10 b). Common technical solutions include the use of commercial slide projectors or enlargers. The condenser ensures proper imaging of the light source onto

the pupil plane of the projection objective. The observation objective is usually a twin of the projection objective, so that the system becomes symmetric. A CCD camera and frame grabber are often used as a recording device. Values for the gratings are of the order of 40 LP/mm, because commercial enlargers can typically resolve these at 60 % contrast. The size of the grating plate is normally less than 100 mm. A typical construction for a projection moiré measurement instrument is presented by Sieczka et al. (1993), for example. The field of view of this instrument is 750 mm x 565 mm and the depth resolution better than 0.3 mm.

Design procedures

The designing of an optical moiré system involves the consideration of many details such as accuracy, field of view, depth of field, system geometry, optics, tolerancing etc. Wegdam et al. (1992) present a method for simulating arbitrary projection moiré systems which is based on the laws of geometric optics and basic formulae for describing the projection moiré system. The authors have implemented a simulation software package which overcomes the limitations of the idealistic mathematical description of an ideal projection moiré system by taking into account influences such as lens systems, object forms, free-formed gratings etc. The results enable one to simulate and predict the performance of real projection moiré systems.

Hauer and Harding (1990) introduced and demonstrated a systematic, well organized approach to designing a moiré interferometer. Their systematic procedure consists of: general specifications, conceptual drawings, preliminary detailed design, final detailed design, physical tolerances of the system components and thermal analysis. This approach can be used to achieve an efficient and complete design for most optical systems. Murakami et al. (1982) studied the setting of the light source for the grid illuminating type of moiré method, and the same authors later presented a procedure for setting up the camera exactly for the grid illuminating type of method (Murakami et al. 1985). Tsuno and Nakamura (1978) examined the accuracy of the projection moiré topography on the basis of geometric optics. Misalignments of the optical elements in moiré instruments cause contour deformations, the error being calculated to depend greatly on the alignment of the grating. The authors altered and compared results based on different parameter values, and showed that errors due to the effects of misalignments are smaller when using projection optics with longer focal lengths and greater magnification.

Performance of the optical moiré technique

When structured lighting measurement methods are applied, the point, line or grid patterns are usually projected onto an object and imaged using a CCD camera. The camera must resolve the displacement of the lines. In such a case, the resolution element of the system can be considered to be the pixel elements of the video camera. When applying an optical moiré method it is not the grating lines that are analyzed directly by the camera

but the moiré contours. The period of the grating is not limited by the video resolution, but rather the ability to make a fine grating and project and image the results. In this manner the moiré technique provides extra leverage. With an optical moiré effect a leverage factor of 10 to 20 over direct grating line analysis with standard video is reasonable in the case of large areas, but over small areas of a few centimetres, the moiré leverage does not gain much advantage without considerable investment in lens performance. As an example in which an optical moiré technique is used to inspect an unpainted car door, the resolution of the data was about 5 μm in depth over an area about 2 metres across. This system gave an optical leverage of about 12 over the direct structured light pattern (Harding 1994).

One capability of optical moiré contouring is that depth information can be averaged over an area of the surface. Methods which measure the contour along a line or use specific points on the object for stereo recognition are sensitive to very small surface areas. The information can be optically integrated over large areas at once by reducing the spatial resolution to that desired (Harding 1996).

Measurement of concave and convex surfaces

When the optical projection moiré method is evaluated from the standpoint of practical use, some problems remain to be solved. The concave and convex regions of an object cannot be discriminated from the fringe patterns formed, and when the experiment is carried out under conditions in which the surface to be measured is out of contact with the grid plane, the fringe index cannot be determined (Murakami et al. 1989). As a solution to these problems, Murakami et al. use fringe patterns formed before and after the object to be measured is shifted in a direction normal to the grid plane.

The slope of the contour can be determined by shifting the phase of the fringe pattern. The most common solution for projection moiré systems is phase shift by means of grating translation (Patorski & Kujawinska 1993). Other possibilities for phase shifters are object translation, use of computer-generated gratings, use of a tilted glass plate or a mirror translator. Dirckx and Decraemer (1990) present a system for automated 3D surface shape measurement based on phase shift moiré. The system sets out from the shadow moiré topography and makes use of four contourograms shifted in phase by translating the object at different z-axis positions. A full-field, 512 pixels square surface shape reconstruction is performed in less than 10 minutes. The resolution of the system is 46 μm, 32 μm and 20 μm along the x, y and z axis respectively. Since the measurement area according to the spatial resolution figures is less than 25 mm, the relation between the depth resolution and field of view is 1:1250.

When using phase shifting there remains an ambiguity if the surface in question has a discontinuous jump (Boehnlein & Harding 1986). As an alternative to phase shifting techniques, the field shift technique described by Boehnlein and Harding (1989) translates the entire projection system instead of shifting only the projection grating. The field shift produces a

phase shift which is proportional to the height of the object and is different from the phase shift where the phase changes uniformly throughout the field independently of the height.

A common technique for solving the hill and valley problem used in classical interferometry is to introduce a bias fringe greater than the slopes encountered, so that all the slopes seen have the same sign. This is equivalent to tilting the object and the measurement unit in relation to each other, or a mismatch between gratings.

Measurement of absolute distances

If absolute distances between the grating plane and the object points are needed or the nonlinearity Δz between the contours is significant, absolute contour order determination is needed. This can be done using reference points, lines or planes in a 3D measurement space, for example, detecting these and computing 3D co-ordinates using triangulation techniques (see Pekelsky & van Wijk 1989).

Xie et al. (1996) introduce a three-map absolute moiré contouring method, a shadow moiré system in which the period of the grating is varied by rotating it, so that the phase of the moiré patterns is changed as well. By selecting suitable rotation angles, three images at different positions on the grating are acquired to obtain the absolute distance from the object to the grating. The results show that the accuracy of the method is better than 10 µm. One measurement takes 3 seconds. The measurement area in the experiments was about 20 mm.

Examples of special implementations

In addition to the conventional topographical moiré implementations, there exist some modifications. Suzuki and Suzuki (1982) introduced recording methods which optically transform cylindrical shapes and record them continuously. The authors have implemented both shadow and projection moiré types of instruments, so that a slit camera is used in synchronisation with an object being rotated about an axis perpendicular to the optical axis of the camera. The slit camera has a film transport arrangement on either the drum or the strip principle. Moiré contours of the cylindrical object can be observed on the film in the form of a strip. The techniques can be applied in cases of continuously rotating components, as may be required for measurement in machine tools or for a single rotation of a component on a turntable.

In the case of projection moiré systems the sensitivity of the system can decrease in regions where the signs of the projection and viewing angles are the same. Another common problem with any moiré system is focusing the projection and viewing systems on the same plane. Harding et al. (1990) present a single lens contouring method to overcome these difficulties associated with small angle moiré methods. They consider a system which uses only one lens, which serves as both a projection and viewing lens. By

this manner, the optical distance to the part and the focus will necessarily be the same for both the viewing and the projection system. Some aberrations of the system are minimized with this one lens approach. A limitation of the single lens moiré approach is the field size that can be addressed in a practical sense. An experimental system was constructed with a field size of about 60 mm and an angle of projection onto the object of 20 degrees. The contour interval was 3 mm. If the depth resolution is assumed to be 1/20 of the contour interval, the relation between this and the field of view is 1:400.

Bieman and Michniewicz (1994) introduce a large-angle incoherent structured light projector, and increase the depth sensitivity of the moiré system by increasing the projection angle. Moiré systems with large projection angles of about 45 degrees are usually built with the principal plane of the projection lens and the plane of the grating perpendicular to the central ray of the projected pattern. This results in curved contour lines, and the resolution of this system varies significantly over the field of view of the camera. The authors describe unique optical geometry for producing coplanar contour lines at a large projection angle. In this arrangement the principal plane of the projection lens is at a 45-degree angle to the principal plane of the viewing lens. Both gratings have the same pitch and are parallel to the principal plane of the viewing lens. The focal length of the projection lens is that of the viewing lens divided by $\cos(45°)$. The magnification of the system is 1 for both lenses. They have reached a depth resolution of 1 μm over a 20 mm field of view. The relation between the depth resolution and field of view is then 1:20 000.

Reid et al. (1987) introduce a modified version of the moiré topography in which the contour interval has been greatly increased, so that in some cases the entire depth of the object lies within one contour. They use a very large contour interval in combination with automatic contour analysis in order to overcome problems such as closely packed contours on steeply sloping surfaces, discontinuities in the surface profile and information losses in a shadowed object area. The large interval used in this study is of the order of tens of millimetres. When phase shifting techniques are used, the contour interval can be subdivided into 100 or 200 increments, enabling sub-millimetre accuracy to be obtained from fringe patterns in which the contour interval exceeds 100 mm. When using the large contour interval, counting of contours is not required, and measurements of the surface co-ordinates have no incremental element.

Nurre and Hall (1992) implemented an experimental inspection system using the projection moiré technique. The system integrates a computer-aided engineering solid modeller with a projection moiré inspection system. The two main hardware components of the system are a CCD camera and a transmissive type LCD array placed in a front of 100 W mercury arc lamp. The LCD array is used for displaying an encoded grid of the object to be inspected. The encoded grid structure is based on the modelled surface with known physical parameters about the system. When an encoded grating is projected onto the object to be inspected, the resulting image of a non-defective part should include parallel straight lines. Instead of using an

integrated solid modeller for making the encoded grating, the grating can be realized by recording a projected grating onto a master piece and replacing the projection grating by the recorded grating. Parallel straight lines are met with when inspecting parts without defects.

2.3.2 Electronic moiré contouring

Electronic moiré contouring refers to the use of instruments in which the forming of moiré contours is largely promoted by electronic components or devices. The contours are not formed as pure optical phenomena based on the two physical grating structures but on the detector or signal level, aided by the electronic components. Some technical solutions based on electronic moiré contouring are reviewed in this section.

Moiré topography using a CCD camera has been implemented by Nordbryhn (1983). A grating pattern is projected on the object by an ordinary slide projector and is imaged from another angle by an interline transfer CCD camera with 380 x 488 image pixels. Moiré contours are obtained between the projected grating and the grid of detector elements in the camera. On the Fairchild sensor CCD 222 vertical light sensitive detector elements are separated by opaque, aluminium-shielded shift registers of approximately the same size as the light sensitive arrays. The contour interval in the experimental tests varied between 1 mm and 10 mm, and the field of view from about 150 mm to 800 mm. This approach gives real-time moiré contouring. The projector and camera must be a long distance away from the object. Otherwise the difference in projection and viewing angle across the object would create cylindrical contour surfaces and not planar ones.

In the scanning moiré method proposed by Yatagai and Idesawa (1981) moiré fringes are obtained by electronic scanning and sampling techniques. The system employs a 1728-element linear photodiode array on a micro-stage as a scanning image sensor, which is moved in a transverse direction by a servo mechanism. The phase, pitch and direction of the scanning lines can be changed, and therefore various contours can be generated immediately. A moiré processor samples the image data in the memory along a virtual grating corresponding to the detection grating in the conventional type of projection moiré topography. The scanning moiré method enables distinction between hills and valleys and the automatic interpolation of moiré contours. The distance from the camera lens to the object was 1.8 metres, the field of view 990 mm x 600 mm and the contour interval 5 mm. If the depth resolution is assumed to be 1/20 of the contour interval, the ratio between the depth resolution and field of view is about 1:4000 (using a field of view of 990 mm in the calculation).

Arai and Kurata (1988) describe a digital image processing method for obtaining a binary scanning moiré pattern. The bias component arising from the distribution of illumination is eliminated from the scanning moiré fringe pattern in order to detect the zero-crossing points of the moiré profile. The

binary fringe pattern is then obtained from the zero-crossing points. The method facilitates 3D automatic measurements using moiré topography, and the results show that it can solve the problems caused by optical irregularities on the surface of the object. The method is reported to be effective in eliminating the influence of irregular lighting, irregular scatter and shading of colour on the object.

A variable resolution video moiré error map system for the inspection of continuously manufactured objects has been developed by Blatt et al. (1990, 1992 a). By generating the moiré patterns in video, it is possible to view the distorted gratings on a test object through a set of gratings that has been distorted by a similar but perfect object. The output is then a set of moiré contours that corresponds to the differences between the two surfaces. This difference or error map eliminates much of the unnecessary information generated in traditional moiré inspection. The system has been applied to damage detection on long, continuous lengths of pipe by means of two side-by-side cameras looking at different sections of the pipe, with the view through one camera filtered with a videotaped recording of an undamaged section of pipe. The measurement set-up involves a cone 25.4 mm high and 50.8 mm diameter with a projection and viewing angle of 21°. The contour interval is 0.3 mm. The extension of this technique to larger targets presents no problem within the limits of the detector system and the optical power of the projector. A depth resolution of about 0.006 times the depth of the target is possible. If the depth resolution is assumed to be 1/20 of the contour interval, the relation between this and the field of view is about 1:3500 (using a field of view of 50.8 mm in the calculation).

In the electronic moiré contouring system presented by Rodriguez-Vera (1994), a linear grating is projected onto the surface of an object. Moiré contours are obtained by comparing encoded information on the object electronically with a reference grating generated by a computer or made by capturing an image from a master object. The moiré inspection system consists of an optical projection, a CCD camera, an electronic apparatus and a computer.

2.3.3 Computer aided moiré

Computer aided moiré methods use the versatility of the computer to manipulate gratings rapidly, thereby benefiting from the ability of the computer to vary the pitch of the gratings rapidly and easily and to shift these gratings in a precise manner. By selecting an appropriate grating pitch it is possible to vary the sensitivity of the method. The simplest computer grating that can be generated consists of an array of zeroes and ones to form a binary grating. A run of zeroes corresponds to a dark line in the grating and a run of ones to the bright line. Moiré contours can be generated by logical operations between gratings. The logical AND of two one-bit binary computer gratings results in moiré contours that are identical in all respects to that obtained by physical superposition of two bar and space gratings.

The logical OR operation gives practically the same result, except that since OR is equivalent to NOT AND the moiré in this case is the negative image of the AND one. The logical XOR provides moiré contours which cannot be obtained using physical gratings, termed logical moiré. Phase stepping techniques show that by using all intensity values, a minimum of three shifted images is sufficient to evaluate the entire fringe pattern. Precise equal shifts in the reference grating are essential for this, and can be provided, with no moving parts, by computer gratings (Asundi 1993). More general grid structures can be produced by an infinitely large variety of moiré fringes. Or in reverse, a specific fringe system can be produced by an infinitely large set of suitable grid pairs (Lohmann & Po-Shiang 1980).

Asundi et al. (1994) propose an experimental projection moiré set-up, as seen in Fig. 11, in which an object is mounted on a rotating plinth driven by a variable speed motor and is illuminated by light from a laser diode. The laser spot is expanded to a line of light using a cylindrical lens mounted in front of the laser. A TDI camera is mounted so that the rotating axis is perpendicular to the TDI scanning direction. The rotating speed and TDI scanning speed must be optimized to record a clear peripheral image of the object. A horizontal grating pattern is generated by slicing the laser line with a grating placed in its path. The laser diode features 100 % depth of modulation, which can be controlled by an external TTL signal. If the laser is pulsed with a pulse duration less than the TDI scanning time for each line, a strip image is recorded in the TDI mode corresponding to the width of the projected line and a vertical grating pattern is generated. The moiré contours are generated by the logical XOR operation or by using the scanning moiré technique, which is facilitated by the camera software. The high speed TDI technique allows high rotation speeds. To demonstrate the feasibility of the method, a can was mounted on a lathe and rotated at 2500 rpm. When using this kind of set-up, the black labels on the object surface were found to absorb the projected light, thereby blocking the defect or shape information. Hence it is preferable to complete the inspection before pasting or painting any labels on the material to be measured (Asundi & Sajan 1995).
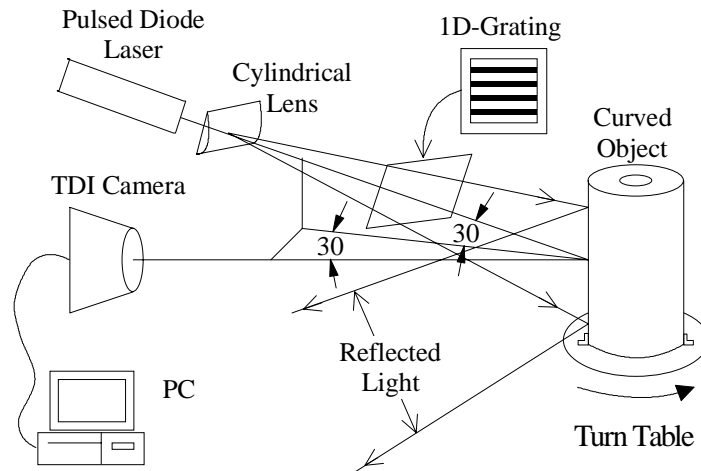
Figure 11. The experimental set-up of Asundi et al. (1994).

2.3.4 Colour-encoded moiré contouring

Harding et al. (1988) describe the use of colour to improve existing contouring techniques. In the case of techniques that include phase shifting, for example, the grating is required to move physically or within software. These techniques suffer from a lack of robustness. Taking multiple images with the hardware uses valuable time, during which the object may actually move and thereby distort the data. It is therefore difficult to get a fast and accurate contour of a part in a real world environment with such phase shifting techniques. The goal of using colour is to develop a means of obtaining one time snapshot of the object that will give all the information required to produce a contour. The authors report results obtained with a red, green and blue camera (RGB). The spectral responses of these channels are preset by the supplier, but there still remains the question as to whether spatial colour variations on the part might prove a major problem. Reflectivity variations are not a problem as long as they affect all three colours in the same way. The use of three colours can produce three usable moiré patterns out of phase with each other during a single exposure.

Hu and Qin (1997) report on a novel moiré pattern colour encoding technique which is able to display moiré patterns with colour sequences that represent fringe orders. The system includes a projector and a black and white CCD camera connected to a frame grabber in colour display mode. Three black and white phase shifted grating images are loaded into the red, green and blue banks of the frame grabber, the phase shift being produced by means of digital image processing. A superimposing colour-encoded image is obtained by using the true-colour display mode of the monitor.

Hoy (1992) introduced a colour digital imaging system for bicolour moiré analysis. This enables orthogonal moiré fringes having distinct coloration to be generated. In conventional moiré analysis applied to dynamic and viscoelastic moiré studies, the U and V displacement fields associated with

the x and y-co-ordinate directions are usually obtained separately, but in many such situations this approach is either impossible or very inconvenient. The generation of bicolour moiré patterns allows simultaneous display of the U and V displacement fringes in red and blue. Two crossed gratings are used, one crossed grating with orthogonal red and blue lines and the other but with black lines in both directions. The result is an accurate, rapid computation of strains without any errors stemming from rotation of the grating. The area of application lies beyond the scope of this thesis, but the principle can also be applied to moiré topography.

Ibrahim and Takasaki (1985) have shown the possibility of determining the absolute order of fringes for shadow moiré topography using a two-frequency technique. They filled black threads at every tenth clearance, or cut off every tenth thread of their grating, so that every tenth order of fringes was marked by intersecting dark or bright lines. Lim and Chung (1988) present a projection moiré topography method using gratings in which colour lines are inserted, so that use of a colour grating allows fringe orders to be determined absolutely without being affected by the separation of two objects being measured, for example. Thus the method does not require the fringe orders to vary continuously.

2.4 INDUSTRIAL APPLICATIONS AND COMMERCIAL PRODUCTS

Suzuki and Kanaya (1988) wrote that moiré topography had reached the stage where techniques were being developed to make this type of measurement method meet practical requirements, and were able to describe industrial applications of moiré topography for shape measurement, flatness measurement and detection of abnormality. The method is suitable for measuring flatness of the order of 0.01 mm to 1.0 mm. The abnormalities detected on the surfaces are partial form variations, aftermarks, dents and other irregularities. Moiré topography can be employed to measure buckling in the pressing of metal sheets for the fabrication of moulded products, and metal formations arising from hot working or welding can also be measured. Other applications include adhesion work, powder moulding and ceramic work, sealing work and safety engineering. Moiré topography can be effect for measuring variations in high-pressure tanks, the reaction towers of chemical plants and transportation pipes. Examples of industrial applications based on moiré topography are presented in Table 2.

Table 2. Examples of industrial applications based on moiré topography.

Application	Reference
Deformation of car panels	(Steinbichler 1990)
Defects in the surface of a panel	(Pat. US. 5,307,152. 1994)
Steel plate flatness measurement	(Sieczka 1992, Sieczka et al. 1993, Matsuo et al. 1990)
Shape of hot steel objects	(Kitamura et al. 1981)
Damage in composites	(Mousley 1985)
Measurement of wing foils, turbine blades or propellers	(Vinarub & Kapoor 1992, Varman 1984, Gåsvik et al. 1989, Clarke et al. 1993)
Undersea mapping and shape measurement, measurement of water waves	(Blatt 1992 b, Grant et al. 1990)
Shape measurement	(Warsaw University of Technology)
Inspection of textile geometry	(Bahners et al. 1994)

The moiré shape measurement technique is useful for repeated measurements, as no targets or surface features are necessary. It gives information about the complete surface rather than selected points. The major disadvantage of using incoherent light in the moiré topographic systems is that the limited depth of focus restricts the information that can be obtained from one view of a component whose surface departs significantly from planar.

Harding and Sieczka (1993), writing about the application of 3D moiré methods to shape recognition, note that changes as small as 0.000254 mm (10 microinches) have been recorded over an area of 25.4 mm x 25.4 mm (one square inch) using moiré techniques. A miniaturized moiré system can be used as a high resolution 3D profiler with a small field of view, including a portable inspection tool, a sensor to encode 3D data into a 2D image and a 3D enhancement accessory for the standard CCD camera.

Miniature 3D moiré instruments have been developed commercially, examples of which are presented in Table 3. These can be mounted on positioning devices such as co-ordinate measuring machines (CMM), layout machines or other arm-based machines, and can be used for 3D part modelling, reverse engineering and automatic inspection in milling processes. They can measure shape parameters such as contours, profiles, flatness, straightness, cylindricity, roundness, slopes and angles, and are able to record hundreds of thousands of 3D data points within seconds.

Table 3. Examples of commercial miniature class moiré products.

Product	Field of view (FOV)	Depth resolution
CADEYES (Air Gage Company 1992) Medar Inc. 38700 Grand River Avenue Farmington Hills, MI 48335 tel. 248-471-2660 fax. 248-615-2971	From 0.9" (=22.9 mm) to 3" (= 76.2 mm)	From 0.00006" (=0.0015 mm) to 0.0003" (=0.0076 mm)
Three Dimensional Cameras, TDC500, TDC550, TDC560 (Dolan-Jenner Industries 1993) JSA Photonics Inc. 2655 B Pan American Freeway, NE Albuquerque, NM 87111 tel. 505-761-3116	From 0.75" (=19.1 mm) to 6" (152.4 mm)	From 0.0005" (=0.013 mm) to 0.013" (=0.33 mm)
EOIS mini-moiré sensors (Electro-Optical Information Systems 1996) EOIS Electro-Optical Information Systems Santa Monica; CA 90406 - 1437	From 1" x 1" (=25.4 mm x 25.4 mm) to 12" x 12" (=304.8 mm x 304.8 mm), resolution and accuracy dependent on surface quality, curvature, discontinuities and positioning system	From FOV/4000 to FOV/2000

3 ON-LINE SYSTEM FOR MEASURING THE FLATNESS OF LARGE STEEL PLATES USING PROJECTION MOIRÉ

This chapter presents specifications and a design for the large-scale on-line automatic flatness measurement system based on the projection moiré technique. The performance of the system is described in Chapter 5.

3.1 MEASUREMENT SPECIFICATIONS

The measurement site at the Rautaruukki Steel plate mill at Raahe is at the end of the mechanical cutting line, before the cold leveller. The standard flatness specification at this measurement site is 6 mm/m (H/L) and a special flatness value of 3 mm/m is often required.

The technical objectives for designing the measurement system were:

❑ depth resolution 0.3 mm (co-ordinate direction z)

❑ depth of field at least 350 mm

❑ minimum length of the wave interval L is 300 mm (see Eq. 1)

❑ maximum measurement time 1 s

❑ maximum plate temperature 100 °C

❑ operating temperature +5 °C - +40 °C

❑ spatial point resolution on the plate 10 mm x 10 mm (co-ordinate directions x and y).

The plates to be measured are up to 3.5 metres wide and may be from 4 metres to several tens of metres long. They may be either stationary or moving on the production line at a speed of 1 m/s. The plates have both diffuse and specular surface properties, which can vary between plate products. The surfaces may also have markings, paintings, dust, water, oil or various kinds of anomalies.

The system is expected to achieve high operational reliability in a hostile plate mill environment, and should measure automatically 99% of the plate products passing the measurement site. It must withstand stray light, dust, vibrations and electromagnetic fields.

The flatness measurements must be seen by the operator both graphically and numerically, and reports on the plates need to be saved for further use.

3.2 DESIGN OF THE FLATNESS MEASUREMENT SYSTEM

3.2.1 System overview

The system consists of three main parts: an optomechanical measurement unit, a DSP frame grabber and a host PC with a user interface (see Fig. 12). Control and data signals are transferred between these three main units.
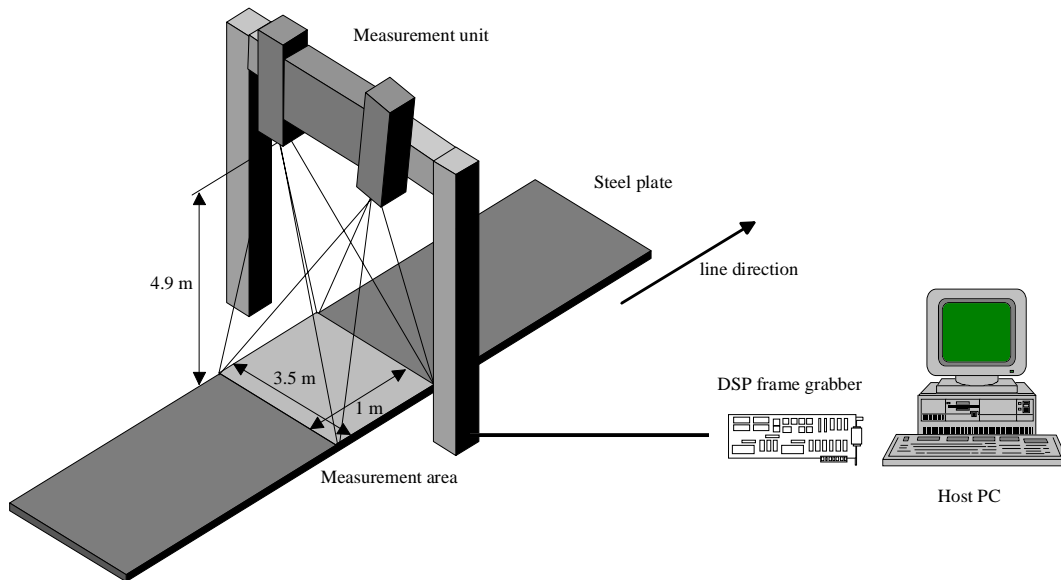

Figure 12. The main parts of the flatness measurement system.

The system is connected to the mill's upper level computer system and process control PC computers via a LAN (Local Area Network). The measurements are synchronized with the material flow on the production line, and the steel plates to be measured are identified by numbers. The plate numbers, dimensions and flatness requirements are read from the mill's database via the LAN, and the measurements can be seen in real time on the user interface. The flatness map of the plate is saved on the hard disc of the host PC for later diagnostic use and its maximum flatness deviation is sent to the mill's database via the LAN. Plate movements on the production line are followed by an ultrasonic switch and rotating encoder. Other necessary interfaces of the system are the power supply and the air pressure connection to cool the illuminator of the optomechanical measurement unit and to make a slight excess pressure around the optical components to eliminate dust. The external interfaces of the system can be seen in Fig. 13.
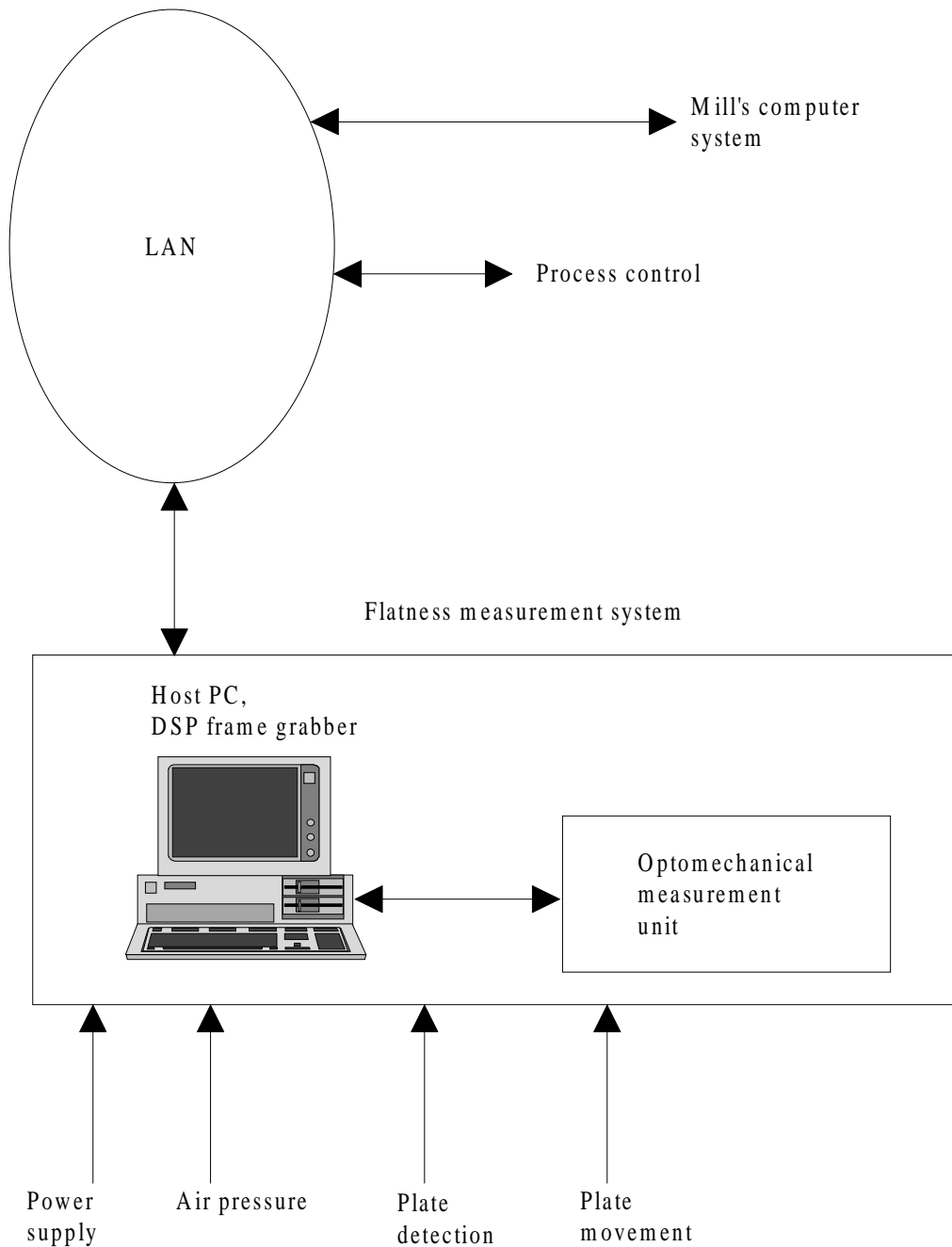
LAN

Mill's computer
system

Process control

Flatness measurement system

Host PC,
DSP frame grabber

Optomechanical
measurement
unit

Power
supply

Air pressure

Plate
detection

Plate
movement

Figure 13. The external interfaces of the flatness measurement system.

The optomechanical measurement unit produces the moiré fringes. The measurement unit is mounted over the production line on a steel frame, the basis of which is isolated from the production line. The distance of the surface of the plate to be measured from the projection lens is about 4.9 metres. The installation of the measurement unit at the plate mill is shown in Fig. 14. Since the variations in background illumination depend on the time of day and season of the year, a shade was designed around the measurement area (see Fig. 14). Moiré contours cannot be seen reliably with this type of system without covering and protecting the measurement area against environmental lighting.

Figure 14. Installation of the measurement unit in the plate mill.

3.2.2 Optomechanical design of the measurement unit

The most critical details of the design work from the optical point of view were the high depth resolution requirement, the large measurement area, sufficient lighting power and mechanical stability.

The projection moiré system can be divided into three subsystems: the projection system, the illumination system and the observation system. The projection system was designed first, followed by the observation system and finally the necessary illumination system. Although each subsystem can be described separately, it should be kept in mind that the separate systems are dependent upon each other. The design process took place iteratively and finally converged upon component selection and positioning. In addition to the optical calculations, some basic laboratory tests were performed in order to verify the results of the theoretical calculations.

To determine the angle between the observation and projection systems, the depth resolution, fringe resolution and grating period on the steel plate must first be ascertained. The depth resolution needed is 0.3 mm, and it was decided that the grating period on the steel should be 1 LP/mm. This is equal to a single line width of 0.5 mm. If the grating pitch on the unfinished steel plate falls below 1 mm, there is an increased likelihood that the grating lines will be blurred and distorted by the grain structure of the steel. It was also assumed that 1/20 of the fringe period can be solved by the image processing algorithm. The observation angle of the system was set at 0 degrees during the design phase. Applying Eq. (10), it can be calculated that

with a system angle of 20 degrees the fringe interval will be 2.7 mm. Thus the image processing algorithm is capable of a resolution of 0.14 mm, which is more than the required depth resolution.

Projection system

The projection system consists of the grating and the projection optics. The periodic structure of the grating is imaged and magnified onto the surface to be measured. Three enlargers for the projection optics were tested in the course of the design work: a 50 mm lens, a 90 mm lens and a 210 mm lens. A short focal length lens would permit a shorter standoff distance but require good off-axis performance. Thus a short focal length lens of 50 mm uses less field angle but needs greater magnification to cover the field width of about 4 metres. Greater magnification implies a need to use a finer grating, and hence greater resolution of the lens.

The quality of the projected grating was evaluated during the design work by means of a white target which was viewed directly with a video camera that enlarged the grating sufficiently to be seen on the video monitor. The contrast of the grating was examined using a video analyzer, which provided a voltage profile for a line of video.

Both the 50 mm and the 90 mm lenses gave results in the experiment that showed a significant degradation in performance across the area needed. The 90 mm lens was the better of the two, going from a contrast of about 60 % at the centre of the field to about 15 % a metre off centre, whereas the image from the 50 mm lens was lost due to noise a metre off centre.

The best performance was achieved with the 210 mm Rodenstock Rogon-ar-s lens, which showed only a slight degradation of grating contrast at the edge of the measurement area. The contrast varied from 60 % to 80 % at the edge of the measurement area.

The standoff of such a system becomes as great as 4.5 metres or more due to the use of a 210 mm lens and the need for a large measurement area of about 4 m. Use of a 50 mm lens or a 90 mm lens would have resulted in a degradation in performance, with significant aberrations, and was not appropriate.

The projection of one line of grating at a magnification of 21x was simulated by using the KidgerOptics design and simulation software. With this magnification a grating period of 0.95 LP/mm can be achieved on the object from 20 LP/mm and a large field of about 4 m can be covered with a grating size of less than 200 mm. As no detailed technical specification of the commercial enlargers was available from their supplier, the simulation was made using an equivalent single lens with a focal length of 200 mm and a diameter of 50 mm. The simulation result, presented in Fig. 15, shows the spread of the line due to lens aberrations.
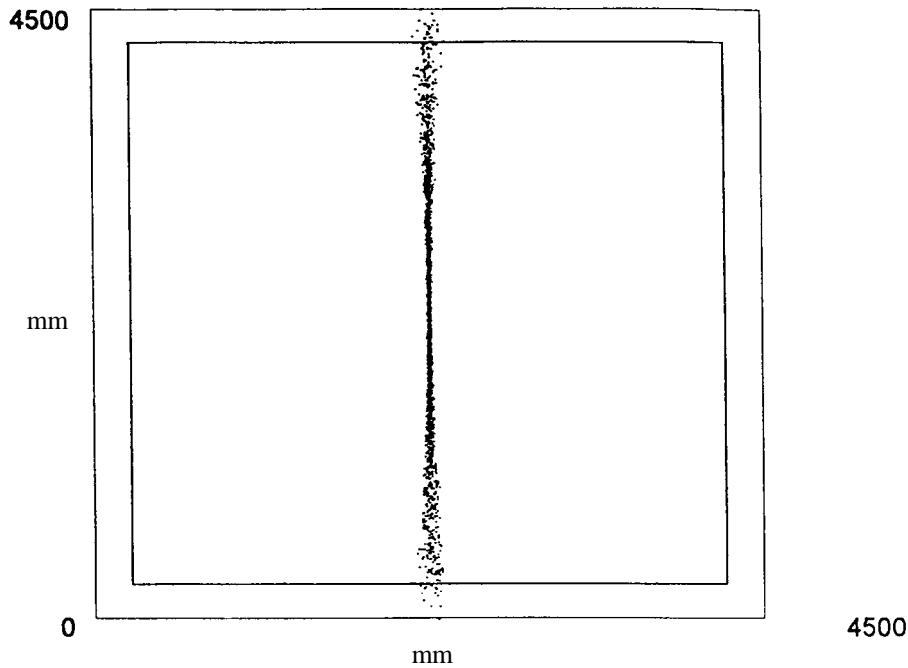
Figure 15. A simulated projection of one grating line on the surface.

A common problem with moiré systems is focusing the projection and observation systems on the same plane because of the curved focus planes of the projection and observation optics (Harding et al. 1990), and the effect of the curved focus planes is particularly obvious in this type of the system with a large measurement area of several metres. These effects were not taken into account during the design of the optical geometry of the system, but the mechanics were designed to allow a slight adjustment of the system angle, projection optics and observation optics during system composition in order to fit the focus planes. Even with a system angle of 15° the depth resolution calculated using Eq. (10) can still be 0.19 mm.

Observation system

The observation system images the object surface together with the projected grating onto a second, detection grating. The observation system could be a twin of the projection system, but this would necessitate a large condenser of about 200 mm, and such a condenser with good imaging properties is not easily found and would be more expensive than smaller lenses.

Instead an enlarger with a focal length of 105 mm and a 40 LP/mm grating was selected, having a magnification of 42x. The grating size of about 100 mm is needed, and this is also the size needed for condenser.

The width of the measurement area was calculated from the geometric optics to be 4163 mm with a standoff distance of 4600 mm. The full advantage of the field of view of the projecting lens is assumed to be used.

47

Illumination system

The illumination of a large measurement area needs to be efficient and uniform enough. The illumination system is based on the traditional projecting system, with a concave mirror reflecting back to the light source and condenser in both the illumination module and the camera module, as seen in Fig. 17. One critical component is a small, high power light source. A life time of one month or more was specified. The light source should be available as a stock product, because it can then be replaced easily and cheaply during maintenance. Also, the need of a special power supply should be avoided. The spectral distribution of the source must fit the spectral responsivity of the camera, and the light must be directed and focused through the optical system. A maximum light throughput will result from the source being imaged into the aperture of the projection lens, and for this a point source is needed.

The power throughput from the point source to the camera detector was calculated on the assumptions that 9 % of the radiation from the source would be collected by the condenser, the concave mirror would increase the radiated power by 3 %, the transmittance of the grating would be 40 % and the steel plate would not absorb light and would represent a completely diffuse surface. The transmittance values of the lenses are based on their technical specifications or on estimates. The values used in the throughput calculation are presented in Table 4.

Table 4. Radiation and transmittance efficiencies used to calculate the power throughput.

	Transmittance or radiation efficiencies (%)
Lamp and mirror	0.12
Condenser	0.92
Projection grating	0.40
Projection optics	0.94
Steel plate	0.0000085
Observation optics	0.94
Detection grating	0.40
Condenser	0.85
Camera objective	0.80
Total	9×10^{-8}

The calculation indicates that the total throughput of the system from the point source to the camera detector is 9×10^{-8}. As an example, a 10 000 lm point source would produce 9×10^{-4} lm, and the illumination on the rectangular 2/3" CCD detector of size 6.6 mm x 8.8 mm would then be 9.5 lx (lm/m^2). This is enough for commercial CCD cameras, which typically have a light sensitivity of about 0.5 lx.

The power distribution over the measurement area, simulated using the KidgerOptics software, is shown in Fig. 16.
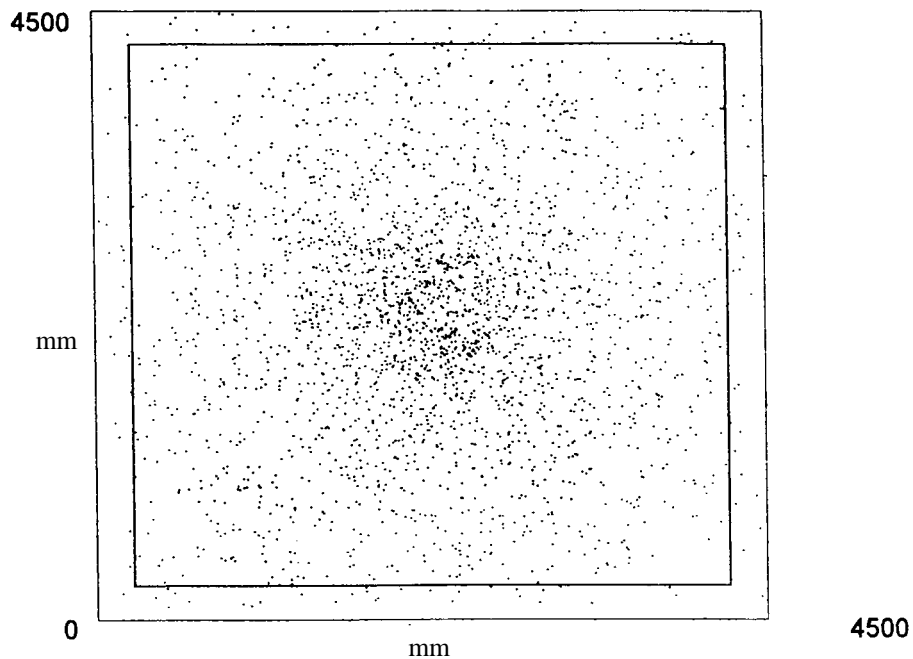

Figure 16. The simulated power distribution.

Various light sources can be considered for the illumination system, e.g. those presented in Table 5.

Table 5. Examples of potential light sources.

Lamp	Luminous flux in Lumens	Lifetime in hours
400 W Halogen	12 200	300
575 W Metal halide	49 000	750
300 W Sodium	34 000	24 000

A high pressure sodium lamp, although bright, is an extended source which is not easily imaged through the optics. The 300 W source is about 100 mm in size and cannot easily be imaged through the 40 mm aperture of the projection lens. The sodium lamp is therefore not an acceptable light source.

The light output of a metal halide lamp deteriorates during its life and its colour temperature changes, in addition to which it needs a special high frequency power supply, as the modulation in the standard 50 Hz power supply can be seen in the camera image. Both 400 W halogen lamps and 575 W metal halide lamps are used in commercial projection light assemblies, the latter being 10 times as expensive.

The 400 W halogen lamp is a small light source with a constant light output over its lifetime. Its filament size is 9.6 mm x 4.7 mm, and DC voltage is recommended for imaging applications. The throughput calculation suggests that its luminous flux of 12 200 lm is enough. This lamp was selected as the light source, although it had a shorter lifetime than required in our specifications. It is capable of illuminating the large measurement area of about 4 m.

Design of the optomechanics

A stable optomechanical construction is necessary in order to achieve high performance and long-term stability under plate mill conditions. It is necessary to adjust the optical components during system composition, after which they should not move beyond their permitted tolerances. Questions of maintenance and environmental conditions also had to be considered in the mechanical design.

The most critical component positions in the system with respect to the projection and observation optics are the gratings. If thermal expansion or mechanical instability causes the optical distance from the projection grating to the projection lens to exceed the depth of focus at the grating, the system will not produce moiré contours and a similar situation is also encountered on the observation side of the system. The stability of the depth of focus was estimated to be kept to 50 μm.

If there is motion between the gratings and the lenses, this will tend to detract directly from the moiré image. A stability of better than 1/20 of the grating period is typically desired, which means that a projection grating of 20 LP/mm should be stable with respect to the projection lens to the extent of 2.5 μm. This does not mean that the position must be accurate to this extent, but only stable.

Approximately similar tolerances were encountered during testing of the other small-scale projection moiré prototype instrument at the steel mill. The depth of focus tolerance was calculated to be 79 μm, and again a grating period of 20 LP/mm was used. The prototype was tested in four parts of the rolling mill, and the results indicated that the mechanics of the optical unit were stable enough. When designing the mechanics of the full-scale system it was decided to use a standard 0.1 mm workshop tolerance. No special bar structures or mounts composed of low expansion steel are used in the mechanics.

The high power halogen light source generates heat in the illumination module, and since the acryl fresnel used as the condenser lens is sensitive to heat, some arrangement is necessary to protect this lens from heat deformation, which would emphasize its aberrations. Air cooling is used for this purpose, and in addition the whole illumination box and all the components are air cooled in order to stabilize the temperature. The camera module has a slight excess pressure inside it to ensure dust protection.

The system was built in the laboratory using a fixed, full-scale mounting frame. This was necessary in order to adjust the mounting position of the whole optomechanical unit, the focus planes of the illumination and the camera module and the illumination itself. Fine adjustments cannot be expected to be accomplished successfully under production conditions in the rolling mill. The optomechanical construction of the measurement unit is shown in Fig. 17. The dimensions of the unit are 2300 mm x 1450 mm x 520 mm (width x height x depth), and it weighs 395 kg.
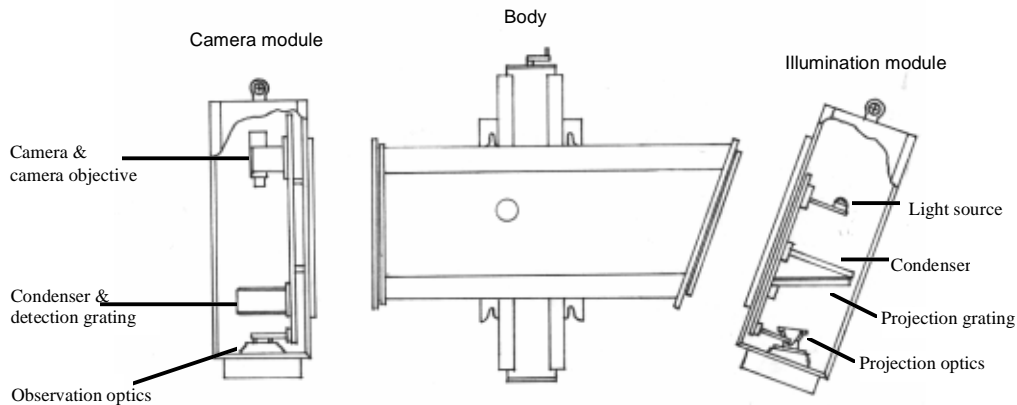
Figure 17. Construction of the optomechanical measurement unit.

3.2.3 Image analysis software

This section presents the algorithm used to interpret the moiré image. The main objectives of the fringe interpretation algorithm and its implementation were a resolution of 1/20, real-time operation and robustness. The algorithm must be capable of interpreting the fringe image despite variation of surface properties within plate products.

The fringe image of the system includes bias fringes achieved by tilting the optomechanical unit and allowing a rotational mismatch between gratings. The purpose of this was to assist both fringe interpretation and visual inspection of the plate products via a monitor image. If needed, the operator can look at the monitor image and observe the straight lines in the case of a flat plate. The use of bias fringes also simplifies the image processing, because mainly vertical and open fringes are imaged with a known carrier frequency, while closed circular fringes can be interpreted as denoting a non-flat plate with no accurate flatness value. Vertical fringes are those which coincide with the line direction and the vertical direction of the camera image.

By tilting the system for bias fringes it is also possible to avoid or reduce the glare from the metal surface. The dynamic range of the camera is set to

cover all the main types of plate products that pass the measurement area. A number of images are taken of each plate as it passes, the imaging process being synchronized with plate movement to prevent overlapping images. These sequential images are later combined to form a set of flatness data for the entire plate.

As noted by Harding et al. (1988), phase shifting techniques suffer from a lack of robustness. Taking multiple images with the hardware uses up valuable time during which the part may actually move and thereby distort the data. In many realistic factory applications the requirement that the part should be held still for three images would greatly limit the application, as the whole idea of the flatness measurement system is to measure moving steel plates. The spatial carrier phase shifting (SCPS) technique is based on the use of a carrier wave and could easily be adapted to this flatness measurement application, too, but it entails a drawback due to unwrapping of the phase and was not selected.

The fringe images on the steel plates have discontinuities due to surface anomalies and markings. As mentioned in Section 2.2, the Fourier method is not capable of providing satisfactory measurements near boundaries or discontinuities, and it is also computationally intensive.

If the phase-locked loop (PLL) technique were adapted to the flatness measurement, it would be applied iteratively to the noisy fringe image on the steel plate, but phase inconsistencies due to the noise would probably be encountered. The iterative process needs careful design of the bandwidth of the PLL and is also computationally intensive.

An intensity-based cumulative phase calculation designed by the author was chosen as the basic method for fringe interpretation. Intensity methods can be expected to have an accuracy of $\pi/20$ of a fringe interval (see Kozlowski & Serra 1997, for example), which is enough for this application. The computation of plate flatness is based on an intensity method which takes advantage of the pixel surroundings, i.e. local image areas. The effects of image distortions on the fringe computation and final flatness values are kept local.

The variation in surface properties between steel plates means that noise is added to the moiré signal. After bounding the plate area the image processing algorithm includes functions for noise filtering, correction of the signal profile and adjustment of the signal level. The design of the filter is based on the known carrier frequency due to the bias fringes, but despite this a noisy image can be considered for feeding to the final phase computation.

A calibration value is used to convert phase information to relative flatness information, a concept that implies that, after imaging the plate area, the flatness information is computed according to its surface with no attention paid to the absolute distance between the plate and the optical unit or to the 3D orientation of the plate.

The algorithm runs in the DSP frame grabber. If needed, the computing power can be increased by adding extra DSP processing units. The block diagram of the algorithm is presented in Fig. 18.
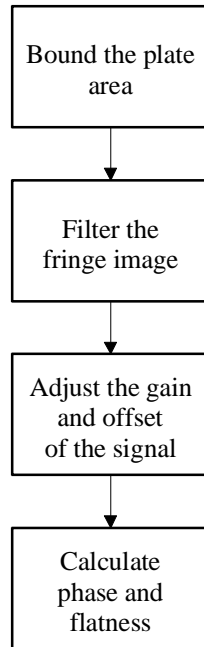
```
┌─────────────────┐
│  Bound the plate │
│       area       │
└─────────────────┘
         │
         ▼
┌─────────────────┐
│   Filter the     │
│  fringe image    │
└─────────────────┘
         │
         ▼
┌─────────────────┐
│  Adjust the gain │
│   and offset     │
│  of the signal   │
└─────────────────┘
         │
         ▼
┌─────────────────┐
│   Calculate      │
│   phase and      │
│   flatness       │
└─────────────────┘
```

Figure 18. Block diagram of the fringe algorithm.

3.2.4 Calibration

Calibration of the system is equivalent to specifying the transformation of the phase information into flatness information. The phase information is expressed in radians and the flatness information in millimetres. The calibration of the system could be based either on theoretical correction or on a reference object, which could be manufactured in a flat or wedge shape, for example. The theoretical correction does not include the influence of aberration and misalignment errors (Kujawinska & Patorski 1993). One practical method is to use a reference object, in which case the calibration takes into account both optical aberrations and mechanical misalignments.

The reference object is manufactured and measured to a known 0.1 mm tolerance using standard workshop tools, and it includes two plane levels with a known height difference corresponding to the phase shift in the moiré image. A technical drawing of the object is given in Fig. 19. One calibration value is used over the whole measurement area, representing the average of the four images of the calibration object located in different parts of the measurement area. The error due to use of only one calibration value is less than 0.1 mm (see Section 5.1). If needed, the measurement area could

53

be divided into subareas, each having its own calibration value. Calibration is supported by the calibration software, and is now performed regularly four times in a year. The calibration object has a diffuse surface without disturbances.
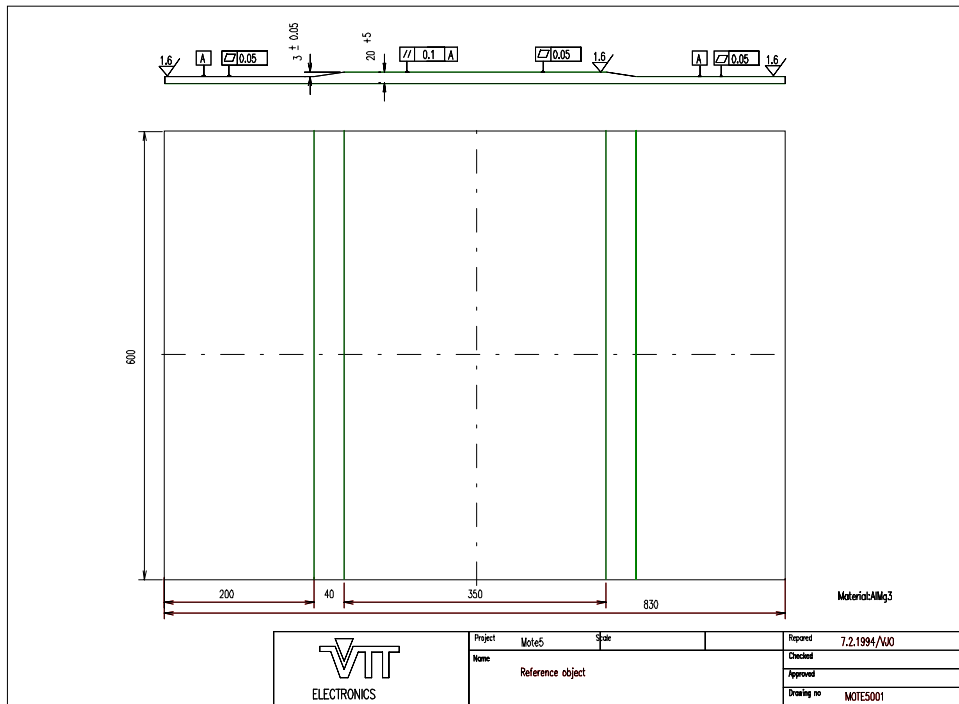

Figure 19. The reference object of size 830 mm x 600 mm.

4 THE MULTIPURPOSE MOIRÉ FLATNESS MEASUREMENT SYSTEM

If a traditional projection moiré method is to be employed for on-line inspection of large objects, many critical details have to be carefully considered. In order to cover a wide measurement area, an optical moiré head for fringe formation needs to be installed several metres away from the object. This is often problematic due to the limited space around production lines and equipment. Reliable, fully automatic fringe interpretation can be based only on high quality, non-distorted moiré fringes. A good fringe contrast is achieved with sufficient lighting power, which is evenly distributed over the object to be measured. The design of a uniform field, high power illumination system for a large-scale projection moiré device is a difficult and demanding task. Furthermore, if the object has a coarse texture or markings, paintings etc. on its surface, these will obviously be seen in the fringe image. These visual surface anomalies can affect the fringe interpretation and reduce the accuracy and reliability of the actual measurement.

This chapter introduces a novel large-scale moiré measurement system. Its robust optomechanical structure, which avoids the tight mounting tolerances seen in current implementations for producing moiré fringes, means that the system will be more applicable to installation in a hostile production environment and at lower cost.

In many industrial cases, additional value could be gained if dimensional measurements, such as width and edge positions could be made with the flatness measurement system. The proposed system offers possibilities for dimensional measurement in addition to flatness measurement. The system is capable of measuring or inspecting width, length and other 2D measures, and to some extent the surface quality of the object.

The main advantages of the new system as compared with traditional ones, and the drawbacks to be minimised or eliminated, are:

❑ The system can be installed close to the object to be measured rather than several metres away. The applicability of close installation depends on the measurement site, but it provides advantages in production lines which have limited space for measurement equipment. No heavy or expensive frame structures are needed.

❑ The mechanical construction of the system is compact, robust and easy to implement, without tight optomechanical tolerances.

❑ The illumination power is better, the profile of the illumination across the object width is more uniform and the contrast of the projected grating is better than in a traditional projection moiré system.

❑ The moiré signal is robust against stray light on the production lines, and if necessary the stray light can easily be blocked by virtue of the compact optomechanical structure of the system.

❑ The effects of the surface texture, markings, impurities etc. on the fringe interpretation can be minimised by using a background image without projected fringes.

❑ The competitiveness of the flatness measurement system is increased by adding measurements such as edges, width or surface quality to the same unit.

The methods used in the novel multipurpose measurement system for flatness measurement, width measurement and visual inspection are described in Sections 4.1 and 4.2, the implementation of the system in Section 4.3 and its performance in Chapter 5.

4.1 PRINCIPLE OF FLATNESS MEASUREMENT IN THE MULTIPURPOSE SYSTEM

Flatness measurement is based on a modular projection system and a linescan camera. The projection system produces a wide collimated light beam over the surface and projects a relatively coarse grating onto it. The linescan camera then produces images of the projected grating lines. Theoretical considerations related to this type of measurement with collimated projection and diverging rays on the imaging side are discussed by Dykes (1970), for example, for the case of the shadow moiré technique. A small section of a grating with pitch p illuminated by a collimated light source at an angle of incidence α is shown in Fig. 20.
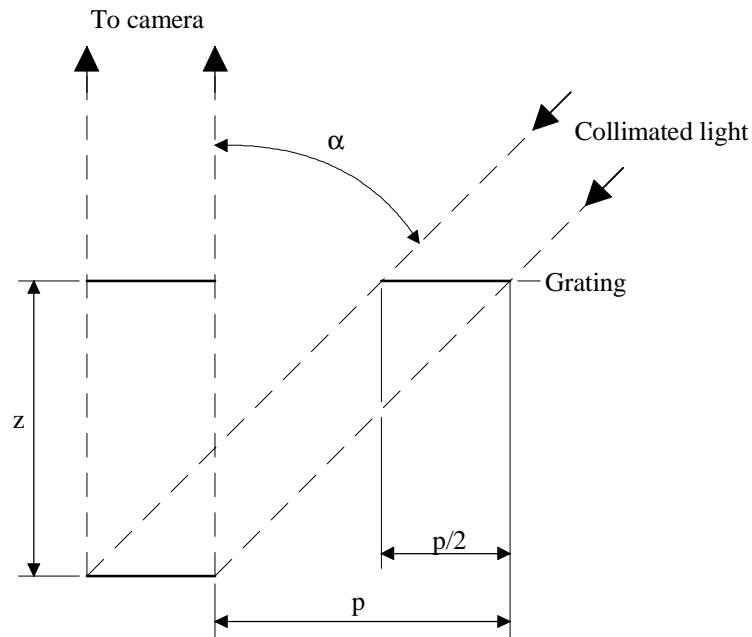
Figure 20. Use of collimated light and a parallel reflection in shadow moiré (Dykes 1970).

The light rays collected by the camera are considered to be parallel to each other and perpendicular to the grating plane. In this case the distance Δz between adjacent contour planes is equal to Eq. (14). This is equal to Eq. (6) when the angle β is set at 0 degrees.

$$\Delta z = \frac{p}{\tan(\alpha)} \tag{14}$$

This situation is not valid when a camera is used for imaging of the shadow of the projected grating. Due to the angle of view of the camera, there is considerable variation in the angles of the light rays collected by the camera. The system uses two beams of collimated light for the projection of the grating and a camera for imaging the shadow of the grating, as seen in Fig. 21. The camera does not see the shadow through the grating, so that no shadow moiré fringes are formed (see Fig. 24).
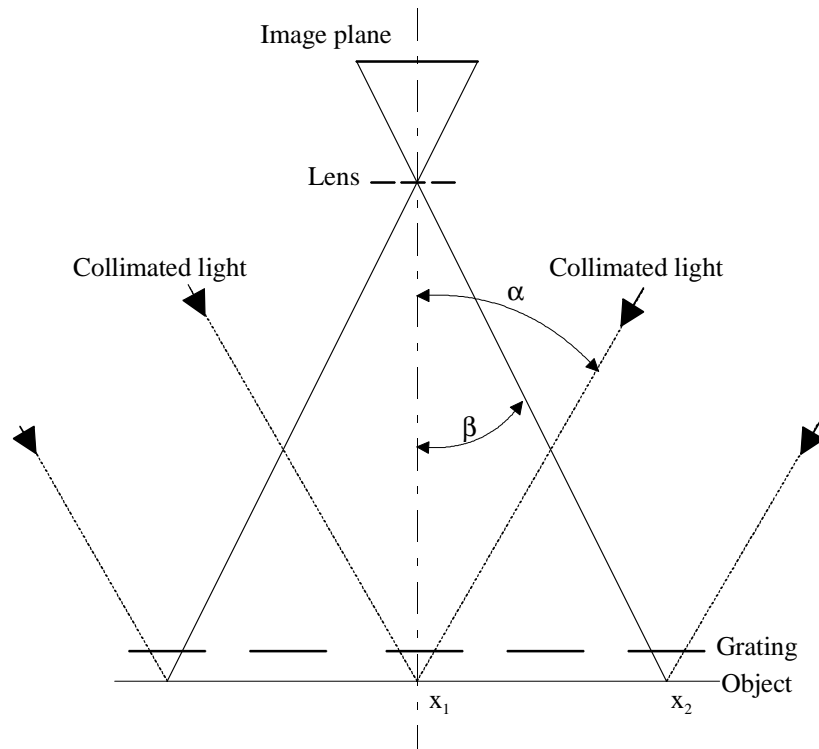
Figure 21. Use of two collimated light beams and a camera for imaging the shadow of a grating.

In this case the depth sensitivity of the system varies over the measurement area according to the angle of view of the camera. The sensitivity in the position x_1 in Fig. 21 can be expressed according to Eq. (14), and that in other positions across the measurement area can be expressed according to Eq. (6) when a continuously varying viewing angle of β is employed. The best sensitivity is achieved at point x_2 on the edge of the measurement area.

The flatness of the object is measured using the logical moiré principle (Asundi 1993). A binary grating with a slightly different period from the projected grating is saved in the computer memory as a reference, and the projected and viewed grating is median filtered using a vertically oriented filtering window of 5 rows x 1 columns. After this the offset of the signal is adjusted and the image is binarized. The final moiré image is formed according to the Eq. (15), in which G stands for the moiré contour image, P for the image of the projected grating, V for the virtual binary grating in the computer memory and x and y for the spatial 2D locations of the images.

$$G(x, y) = \left| \, P(x, y) - V(x, y) \, \right| \tag{15}$$

The moiré image G is then averaged row by row to form a wavy moiré signal. Vertical straight bias fringes are seen in the case of a flat object.

4.2 INTEGRATION OF WIDTH MEASUREMENT AND SURFACE QUALITY INSPECTION

Since the novel multipurpose system captures grey level images of planar objects, it offers possibilities for integrating width measurement and other measurements such as length, edge camber and out-of-squareness in the same unit. Visual surface inspection is also possible to some extent.

Width measurement

Other measures besides flatness are necessary in the case of steel plate or strip products. The SFS-EN 10 029 (1991) standard for "hot rolled steel plates 3 mm thick or above - tolerances on dimensions, shape and mass", for example, assumes that several measurements can be carried out: thickness, width, length, edge camber, out-of-squareness and flatness. Width should be measured perpendicular to the major axis of the plate, while length is the length of largest rectangle contained within the plate. The edge camber value q is the maximum deviation between one longitudinal edge and the straight line joining the two ends of this edge, and is measured on the concave edges of the plate. The out-of-square value u is the orthogonal projection of one transverse edge on one longitudinal edge. The measuring of edge camber, out-of-squareness and flatness is described in Fig. 22. It is evident that an automated system for performing many of these measurements simultaneously in real time without manual intervention would be beneficial to steel manufacturers.
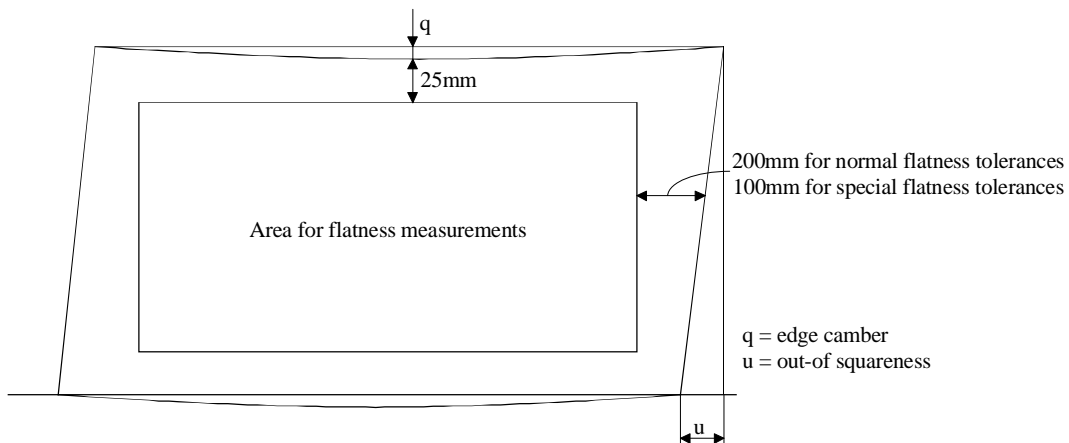

Figure 22. Measuring of edge camber, out-of-squareness and flatness of a hot rolled steel plate (SFS-EN 10 029).

Width gauging by reflection is implemented in the multipurpose flatness measurement system through imaging of the width of the steel strip or plate by the camera objective on a linear detector array. A resolution of the order of 1 mm over a strip 1 m wide can normally be achieved with this type of system (Cielo 1988), but higher resolutions can be obtained in theory by interpolating between adjacent elements and subsequently applying a convenient threshold to the continuous curve thus obtained. In practice

signal fluctuations resulting from variations in the illumination distribution, lens aberrations, sensitivity non-uniformity across the detector array and variations in the camera to strip distance, leading to parallax errors, limit the accuracy in this configuration. The illumination of the sheet must be chosen carefully. Several lamps at a non-specular incidence angle should be distributed along the strip width to produce well balanced illumination across the sheet, resulting in a uniform signal across the illuminated line arrays elements. Care must also be taken to ensure a dark background on each side of the strip edges (Cielo 1988). The principle for measuring the width of plate or strip products is presented in Fig. 23.
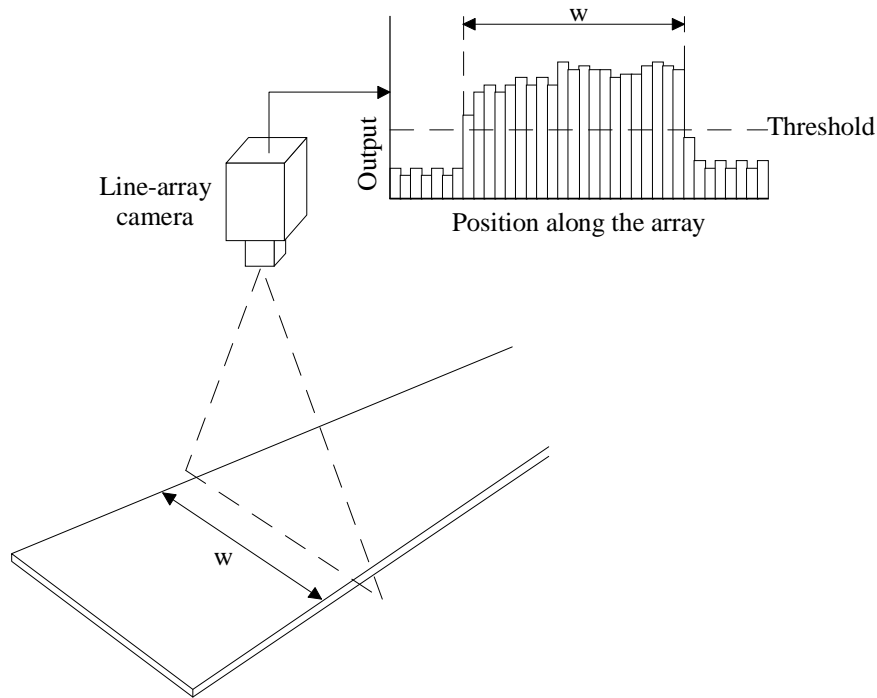
Figure 23. The principle of width measurement.

Width measurement is based on location of the edge of the strip or plate product. Edges and their location play a central role in the study of the metric fidelity of digital images. There are a number of techniques available that can be used for edge location if pixel accuracy is desired, but it is possible to determine the edge location to subpixel accuracy by examining the transfer function of the digitizing equipment and the output pixel values. Tabatabai and Mitchell (1984) introduced an analytical definition of edge location and an approach which is based on fitting an ideal step edge to a set of empirically obtained 1D edge data. The method is easy to derive in closed form, which in turn reduces the computational load. The method is invariant to multiplicative and additive changes in the data. This is important, because both optical and image processing operations can scale and shift the data. The edge locations used for width measurement in the multipurpose flatness measurement system are computed to subpixel values based on this method.

Surface inspection

The industrial needs for surface inspection are of two types: measurement of average surface roughness characteristics and detection of abnormal surface characteristics in localized areas, i.e. surface defects (Cielo 1988). There exist inspection systems which are dedicated to be used for the inspection of steel strip or plate products. The detection of surface defects requires full inspection of the product, and specially designed illumination and viewing, very high spatial resolution and high data rates supported by powerful computing are often needed.

The multipurpose flatness measurement system is not specially designed or optimized for surface quality inspection, but rather the inspection of surface quality is often considered a secondary task to be performed at sites of flatness measurement. The primary task is to measure flatness, and possibly other 2D dimensions of the plate products, but clear surface anomalies such as holes or coating defects can be detected using a background image within the limits of the spatial resolution of the system. The system presented here provides opportunities for the development of an application-specific image processing algorithm for surface quality inspection.

4.3 EXPERIMENTAL SYSTEM

The principle of the experimental multipurpose laboratory flatness measurement system implemented at VTT Electronics is presented in Fig. 24. It is composed of a projection system with modular lighting units and a grating, a linescan camera and a computer.
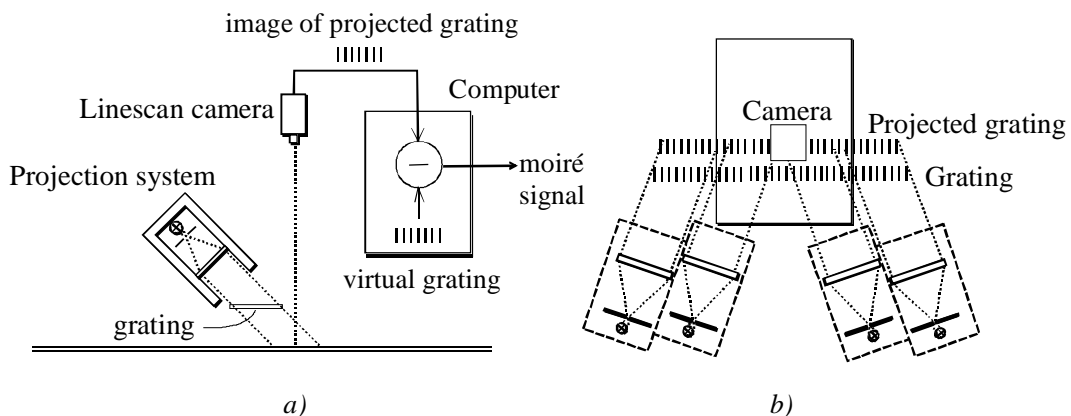

Figure 24. a) Side view of the flatness measurement system and b) a view from above.

The use of a collimated light beam is reported in many papers to limit the size of the measurement area. As a solution to this problem, parallel and modular lighting units are used in the experimental system, each unit

61

consisting of a slit and a standard fresnel lens used for producing a collimated light beam. The slit is oriented according to the grating lines and is positioned at the focal point of the fresnel lens. The use of a slit and a standard fresnel lens means that the collimated light beam is produced in only one direction. A focal length of 610 mm is used for the fresnel lens in this system. The structure of the illumination unit is shown in Fig. 24 b). A halogen source with a background reflector can be focused on the slit, or alternatively the area of the slit can be filled with optical fibres and light can be directed to the slit by means of these. The size of the slit is 5 mm x 100 mm (width x length). Side views of these two alternative types of illumination are presented in Fig. 25.
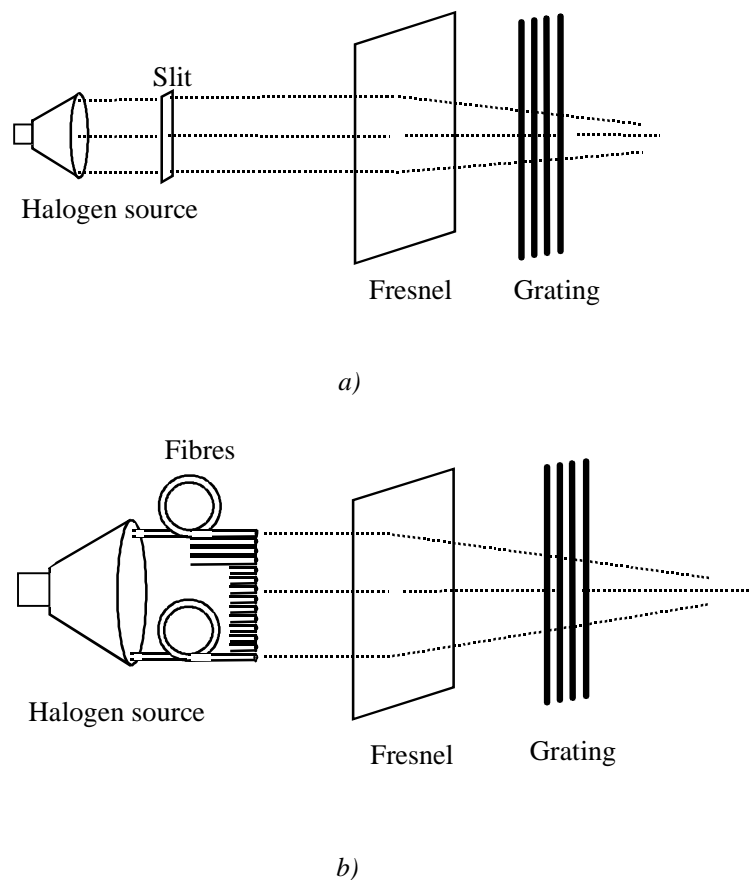
Figure 25. a) Side view of the halogen source focused on the slit and b) a slit filled with fibres used to direct the light.

Each lighting unit has its own 50 W halogen source and illuminates an area of 380 mm x 120 mm (width x length) with a measured white light varying from 400 lx to about 1000 lx. No noticeable heat is generated by these sources. The lifetime of the sources is 3500 hours, or almost five months.

A coarse projection grating with a 1.5 mm line width is used between the collimated lighting units and the surface to be measured. The collimated lighting units are set to projection angles from 10° to 20°, and the grating is

produced graphically, which is cheaper and simpler than the coating process used in the case of fine optical gratings with a period of 10 LP/mm or so.

The projected grating is viewed by the linescan camera, which provides a high spatial resolution across the object and can be synchronized to the speed of the production line. High spatial resolution is necessary in this kind of multipurpose vision system, because grating lines, plate edges and surface defects all need to be resolved by a camera. The pixel resolution of the camera must be scaled so that each grating line is covered by two or more pixels. A Dalsa colour linescan camera with 2048 pixels is used in the experimental system, and the width of the measurement area is 1200 mm, so that the width of one pixel is 0.6 mm.

Use of background illumination and colours

In the case of the flatness measurement system presented in Chapter 3, the effects of paintings, markings or other surface anomalies on the fringe interpretation are reduced by spatial filters during signal processing. In the case of markings made on the surface of the steel plate at the same spatial frequency as the moiré fringes, for example, the filter allows these markings to be fed to the final phase computation and to increase the noise of the final flatness measurement.

The use of colours and background illumination makes it possible to minimize the effects of surface anomalies in the final fringe interpretation. The background image can also be used for width measurement and surface quality inspection. A flatness measurement system with background illumination and the use of colours is presented in Fig. 26.
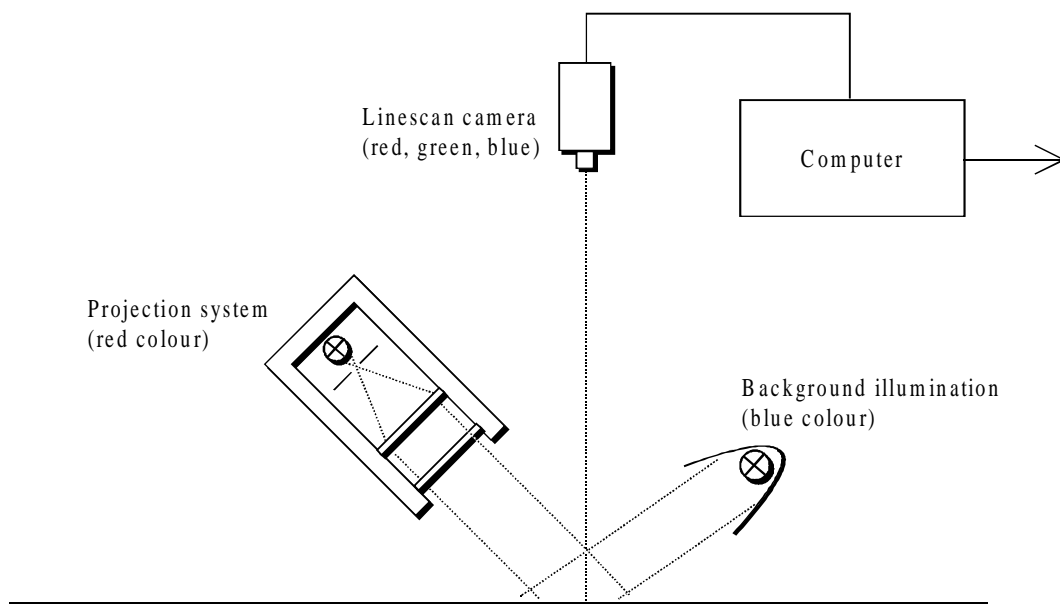

Figure 26. Principle of flatness measurement with background illumination and the use of colours.

In Fig. 26 the camera views the surface and simultaneously detects the image of the projected grating together with the surface of the plate and the image of the surface of the plate without any grating. These two images are separated on the basis of colours. The background lighting produces a blue light adapted to the spectral responsivity of the blue channel of the linescan camera. A red spectral filter is placed in front of the slits in the projection system and the grating image is adapted to the spectral responsivity of the red channel of the linescan camera. The green channel of the camera forms a safety margin between these red and blue images. The blue channel includes visual information regarding the surface of the steel plate, and the surface anomalies are detected and located on this image. The detection takes place columnwise. If the local pixel values differ from the slowly moving average column values, the pixels concerned are thresholded and labelled for correction. These localized defects, markings etc. are then corrected in the red channel grating image. The correction is again made columnwise manner, which is also the principal direction of the grating lines. At the position of the labelled pixel, a new pixel value is estimated using previously detected proper grating lines and their direction. The experimental system is illustrated in Fig. 27.
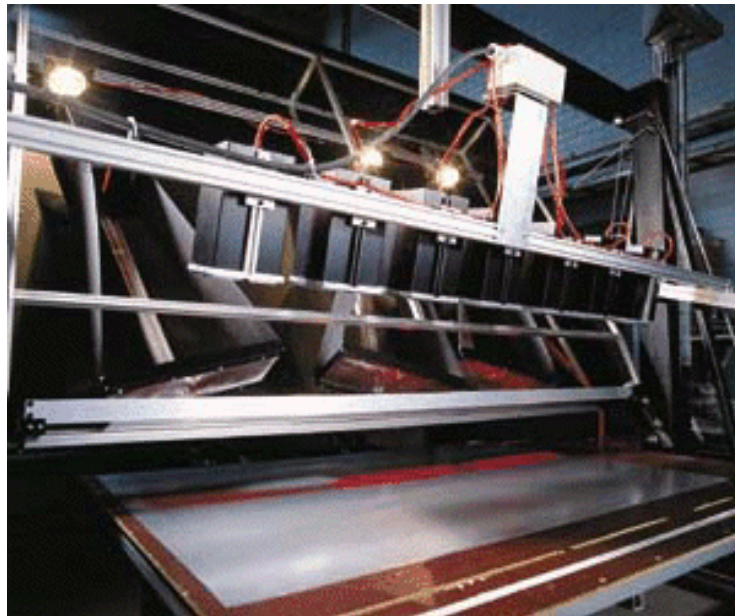

Figure 27. Experimental multipurpose measurement system for use in the laboratory.

5 PERFORMANCE EVALUATION

The characteristics of 3D optical measurement systems include resolution, repeatability, accuracy, field of view, depth of field, standoff and measurement time, some of these being functions of the measurement range. Other characteristics of interest when comparing systems are of course cost, calibration requirements, physical size, environmental requirements, target material dependence etc. Evaluation and comparison of the characteristics and performance of systems is important for a developer, in order to know the state of the art, for a manufacturer, to be sure of the quality of his products, and for a potential end user, to make choices between alternatives (Paakkari & Moring 1993). Besl (1988) uses a figure of merit to describe the performance of a 3D measurement system based on its working volume, accuracy and measurement time. The problem he discovered is that manufacturers specify the same factors in quite different ways, due to the test conditions, properties of the scene materials and perhaps even some conscious underrating or overrating.

A method and environment for evaluating the performance of range imaging sensors has been developed by the author (Paakkari 1993). This approach lies somewhere between the calibration methods and the application-specific alternatives, and can be used to determine the basic performance properties of a sensor not only with one fixed test object but with objects of several types having different surface geometries and materials. The environment consists of several reference objects, and procedures were developed for processing and analyzing the information acquired in order to provide an accurate, illustrative output of the results. One of the key features is that no special targeting of the sensor is required for the reference shapes because alignment of the reference geometries and acquired data is taken care of by the software. An iterative least squares method was chosen for alignment purposes, because good accuracy and reliability were needed but the speed of execution was immaterial (Paakkari 1993).

No common or standardized practice exists for performance evaluation. The reference objects used in the above method were not appropriate for testing the present large-scale flatness measurement system, as large steel plates with a shape accuracy of 0.1 mm would have been needed. In addition they would have had to be flat in shape or otherwise suitable for the algorithms used in the evaluation method, and their shape would have had to remain stable in regular checks. Reference objects of this kind would have been impractical to handle and store during tests both in the laboratory and in the factory. An application-guided evaluation related to the specific flatness measurement problem was therefore performed here according to a prearranged test plan, being aimed at assessing factors such as signal quality, repeatability, depth resolution and measurement area.

5.1 PERFORMANCE OF THE OPTICAL PROJECTION MOIRÉ FLATNESS MEASUREMENT SYSTEM

The performance of the system presented in Chapter 3 was studied under both laboratory and factory conditions. The tests were performed according to prearranged plans.

Quality of the moiré signal

Two steel plates of size 2 m x 2.5 m were placed in parallel in the measurement area, together covering an area of 4 m x 2.5 m in the laboratory hall. An example of the moiré image and the profile of the moiré signal are seen in Fig. 28. The horizontal profile was taken from the middle of the image. As noted in Section 2.2, the unknown to be extracted is the phase information, not the fringe contrast or intensity.

For a visual interpretation of the plate image, the flatnesses of the sample plates were measured using a vertical straight edge. The measurement locations and the flatness deviations can be seen in Fig. 29, where the black spots and their co-ordinates are points where the straight edge was touching the sample surface. The numbers without parentheses indicate depth deviations from the straight edge in millimetres, and the locations of these numbers in Fig. 29 indicate approximately the locations of the depth deviations along the straight edge and can be compared with the curved moiré fringes seen in Fig. 28.

This visual interpretation suggests that a depth deviation of less than 1.0 mm will be seen as a curved fringe. The moiré image can be used by the operators as a visual aid.
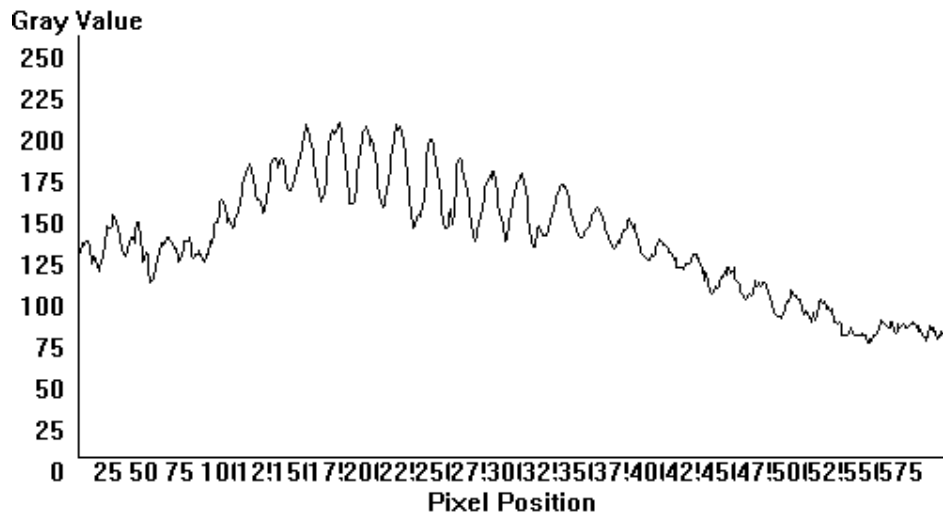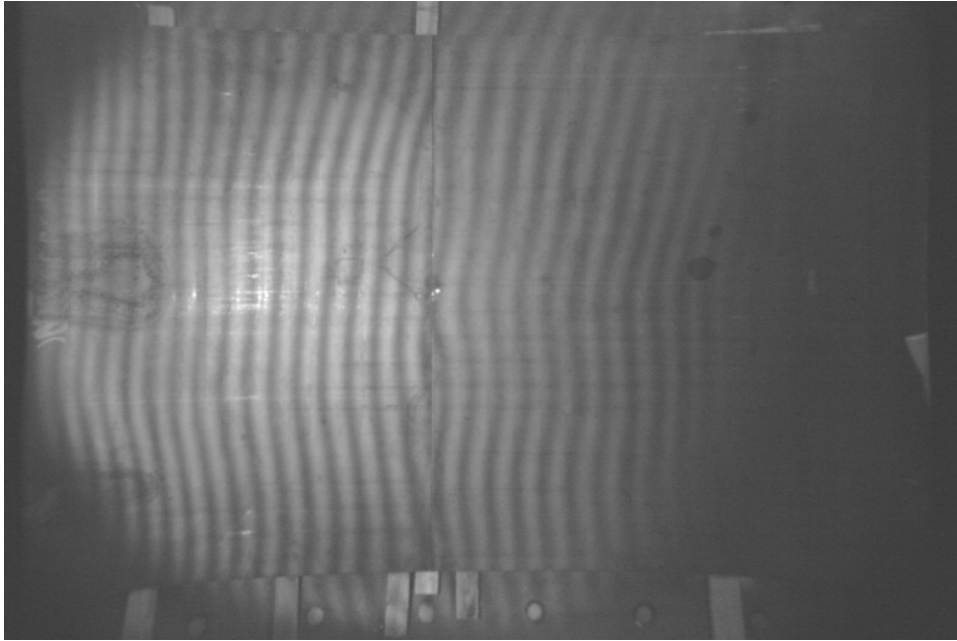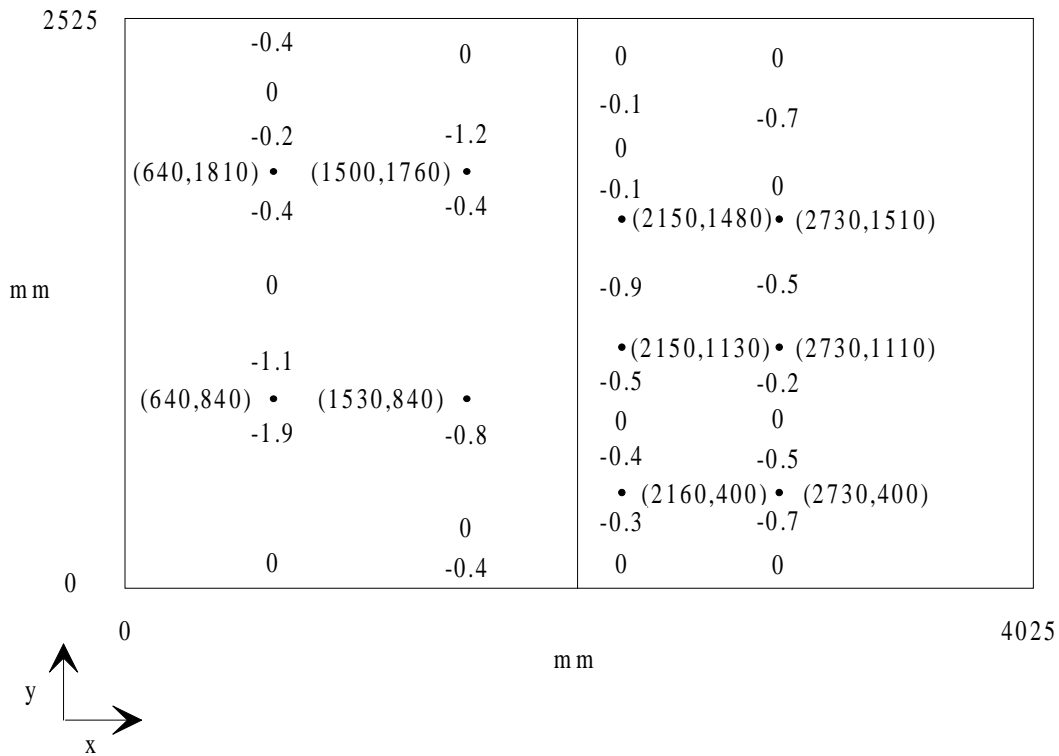
Figure 28. Example of a moiré image and a profile as obtained in the laboratory.

Figure 29. Flatness deviations in the sample.

Calibration

The system is calibrated using a specially manufactured reference object having two plane levels, as seen in Fig. 19. This is placed in four locations at equal intervals along the width of the measurement area of size 3.5 m x 1.0 m (width x length) and 0.5 m up from the lower edge of the area. The fringe deformations on the reference object are interpreted by the algorithm used for the flatness measurements. The average of these four calibration values indicates that a +1.0 mm depth deviation corresponds to a fringe deformation of 9.06 pixels.

Repeatability and depth resolution of flatness measurement

Repeatability was assessed by measuring the calibration reference object 12 times within the measurement area at the steel mill, as three sets of four measurements. Changes were made to the measurement system between sets and a different calibration value was used within each set. The calibration value is the average of four measurements of the set and expresses the relation between a 1 mm height deviation and the corresponding phase shift in the moiré image (mm/ϕ). Calibration values, i.e. phase shifts corresponding to 1 mm height deviations, were also computed based on individual measurements and compared with the average value of the set of four measurements. These deviations in millimetres and locations of the calibration object in the measurement area are presented in Table 6.

Table 6. Measurement of the calibration object in the measurement area.

Number of measurement	Location of the calibration object in the measurement area	Deviation in millimetres within the set of four measurements
1	▮□□□ ↓ line direction	-0.01
2	▮□□□ ↓	0
3	▮□□□ ↓	-0.03
4	□□□▮ ↓	0.04
5	▮□□□ ↓	0.01
6	▮□□□ ↓	-0.03
7	□□□▮ ↓	0.01
8	□□□▮ ↓	0.01
9	▮□□□ ↓	-0.06
10	□▮□□ ↓	0
11	□□▮□ ↓	0.1
12	□□□▮ ↓	-0.05

The standard deviation (σ) of these 12 measurements was 0.043 mm. If a normal distribution is assumed, 2σ will be 0.086 mm and 95.5 % of the random measurements will lie between -2σ and $+2\sigma$. The repeatability of the flatness measurement is 0.086 mm. The depth resolution, i.e. the smallest flatness deviation which can be reliably detected, can be deduced from the normal distribution of the random measurements. If the flatness deviation in the object is 4σ, which amounts here to 0.17 mm, it can be reliably detected.

The practical performance of the system was evaluated under production conditions using steel plates passing the measurement site. Eight steel plates of varying thickness and surface properties were selected and measured manually as a reference, their flatness being measured using a straight edge along the longitudinal axis. The discrepancies between these manual measurements and the flatness results based on moiré contours were in the range 0.3 mm - 2.0 mm, or 0.5 mm - 1.5 mm in the case of three plates with dark, non-reflective surfaces. Conversely, it was the one plate with a highly-reflective surface in which the difference was 2.0 mm. A plate having white markings on it was also measured, and this, too, gave a difference of 2.0 mm. The use of manual measurements as a reference is somewhat problematic, however, as the exact positions of the supporting points and measurement point of the gauge are not always known, and in any case longitudinal measurements fail to detect the transverse curvature of the plate.

The representatives of Spectra-Physics VisionTech Oy have measured five moving steel plates twice using the optical projection moiré system and compared the two sets of results. The difference was -2.5 mm in the worst case and -0.7 mm in the best case, the average for the five plates being 1.3 mm.

If the moiré contours are distorted by markings or bad surface quality, for example, the performance of the flatness measurement system will deteriorate. The algorithm has later been modified so that the system will give results only for plate areas where the fringes can be detected reliably and are not broken or scattered, and these results will be accurate, but an operator is needed to check the flatness measurement map and assess the flatness of the areas not measured. It is thus the operator who decides whether the plate being inspected fulfills the specified flatness value of either 6 mm/m or 3 mm/m. Differences between shifts in the targeting of plates for levelling are nevertheless significantly reduced.

The objective for depth resolution was specified in Section 3.1 as being 0.3 mm, which, using the calibration result mentioned above, corresponds to a fringe deformation of 2.72 pixels. Since the average pixel size on the steel plate is 5.6 mm, this implies 15.2 mm on the steel plate. This deformation can be seen visually and computed by the flatness measurement algorithm. The test results indicate that the system can resolve specified flatness deviations of 0.3 mm.

Other performance values

The other performance values evaluated are presented in Table 7.

Table 7. Performance of the flatness measurement system.

Performance factor	Specification	Result
Depth of field	350 mm	520 mm
Measurement area	3.5 m wide and from 4 m to several tens of metres long	3.5 m x 1 m, sequential non-overlapped images are captured
Spatial point resolution on the plate surface	10 mm x 10 mm (x and y directions)	5.6 mm x 5.3 mm
Usability	99 % of plate products must be measured	100 %, based on the discussion with the production personnel

Experiences

The system is now in continuous operation, and has remained mechanically stable for three years. No optical or mechanical adjustments have been needed during operation, and no dust has penetrated inside the illumination or camera module.

The flatness reports on the plate products have been saved and analyzed for use in joint negotiations between the steel company and certain clients.

5.2 PERFORMANCE OF THE MULTIPURPOSE FLATNESS MEASUREMENT SYSTEM

The performance of the multipurpose flatness measurement system was tested under laboratory conditions, employing a prearranged test plan with different types of steel plates of varying surface quality and thickness.

5.2.1 Performance of the flatness measurement function

Quality of the moiré signal

The quality of the moiré signal was assessed with steel samples of different types, including rolled steel, hot galvanized steel, electrically galvanized steel, plastic-coated coloured steel and a steel sample from the pickling line. A paper sample was also used. The quality of the moiré signal was excellent or good in all cases except for a green plastic-coated plate with a small regular pitted texture on its surface, where the pits acted as small mirrors distorting the quality of the projected grating. Two examples of the normalized moiré signal, using a paper sample and hot galvanized steel, are presented in Fig. 30. The paper sample can be regarded as representing a fully diffuse surface and the hot galvanized steel plate as an almost entirely specular surface. The projection angle was 15° in each case.
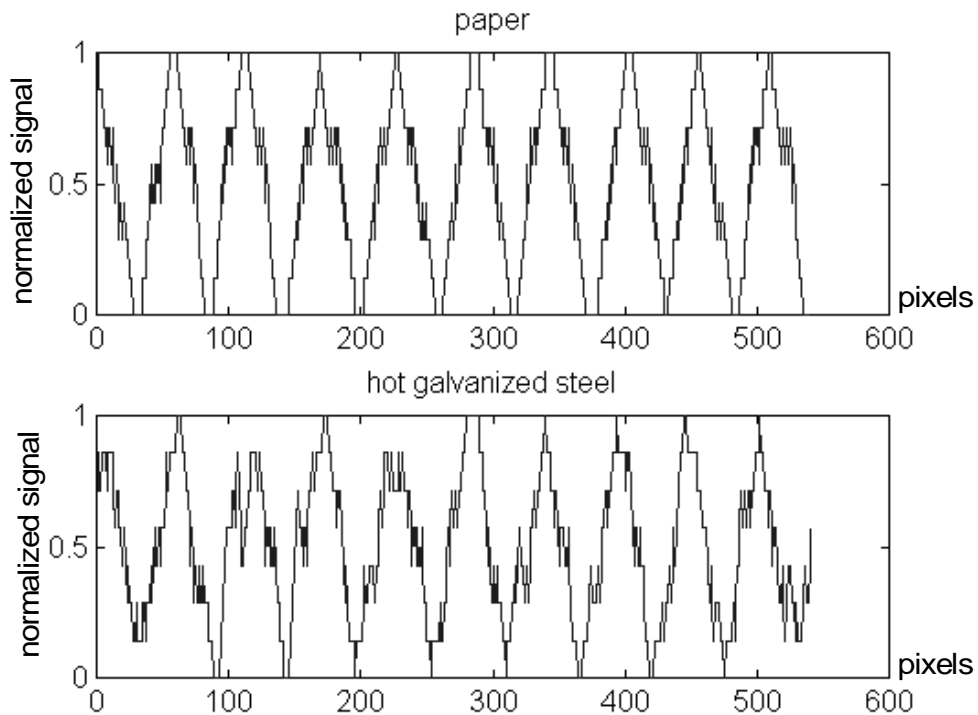

Figure 30. Moiré signals for a paper sample and a hot galvanized steel surface.

When the signal profiles presented in Fig. 30 are compared visually with that presented in Fig. 28, the quality of the signal can be seen to be better. The contrast in the moiré contours is better and the wave form of the signal can be detected more easily. It is then probable that the fringe algorithms will also be able to interpret the signal more reliably and accurately. Signal quality is also seen to remain good in the case of a diffuse surface or an entirely specular surface.

The effects of surface anomalies on the moiré signal can be minimized and the quality of the signal improved by the use of colours and background illumination. An example of minimization of the effect of writing painted on the rolled steel is presented in Fig. 31.
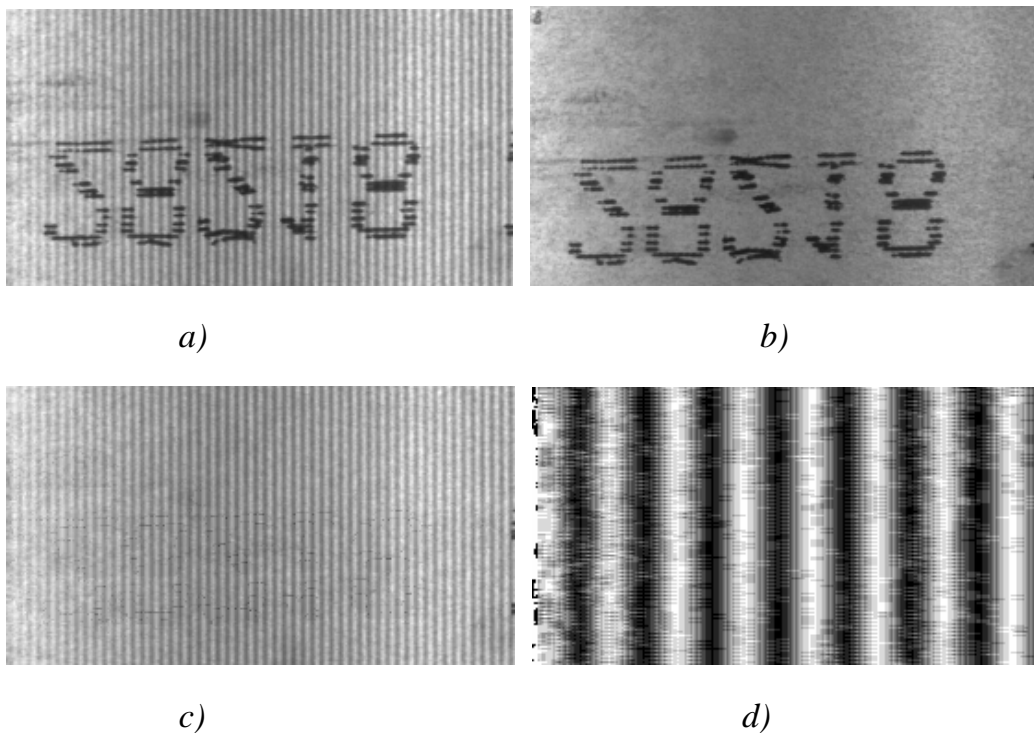

a) *b)*

c) *d)*

Figure 31. Minimization of the effect of words painted on the rolled steel with respect to a) the projected grating image, b) the background image, c) the corrected grating image, and d) the final moiré image.

Disturbances of many types are present under factory conditions that cannot be simulated reliably in the laboratory, but it was possible to simulate the effect of stray light using the prototype system. Two 55 W compact fluorescent lamps, each producing 4800 lm, were placed at a 45° angle of incidence 300 mm away from the measurement line, and it was found that the moiré signal generated by the system was able to withstand this strong stray light. The combined illumination level of the red projection system and the blue background illumination is about 2000 lx. As an example, the profile of a moiré signal for the electrically galvanized steel sample is presented in Fig. 32 without stray light and with very strong stray light of about 13 000 lx, more than 30 times the level measured at the plate mill.
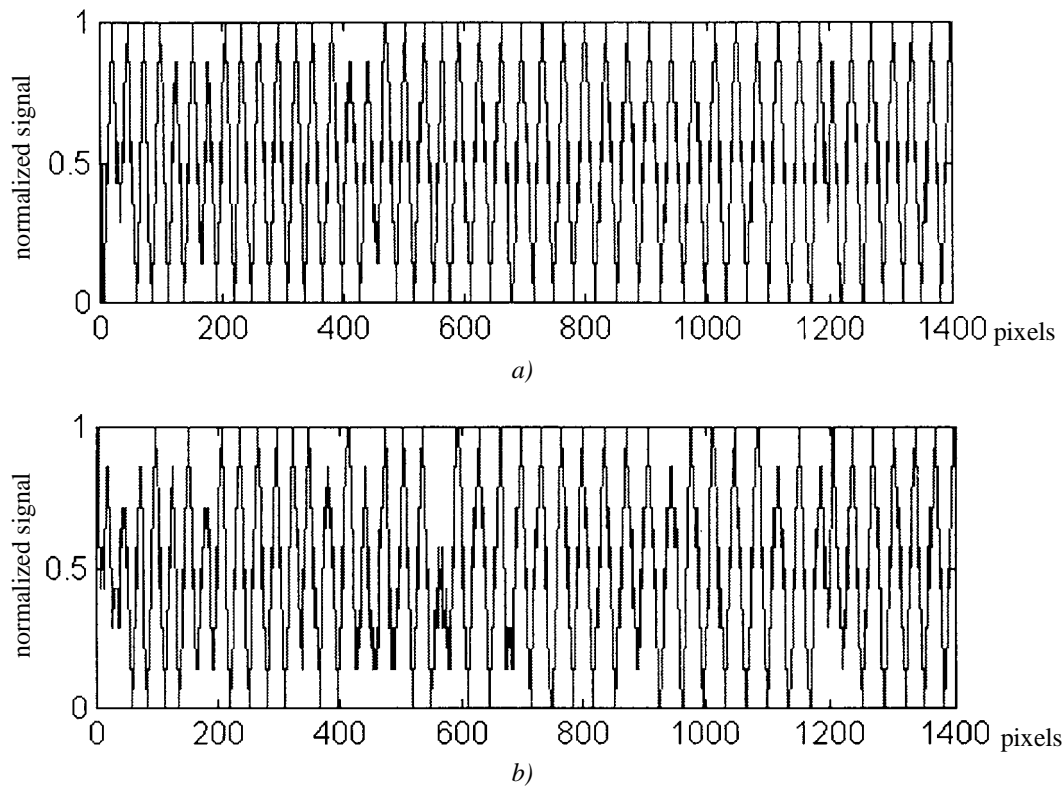
Figure 32. Effect of strong stray light on the electrically galvanized steel a) no stray light and b) strong stray light of 13 000 lx.

Repeatability and depth resolution of flatness measurements

After the moiré image has been formed according to Eq. (15) and averaging has taken place, the same image processing algorithm can be used as in the case of the optical projection moiré system (see Section 3.2.3). The repeatability of the flatness measurement of the optical moiré system has been shown to be 0.086 mm (2σ), equal to a phase shift of 0.78 pixels.

The repeatability of the novel flatness measurement system has not been tested, but it can be estimated. If the same algorithm as described in Section 3.2.3 is used and a moiré signal of better quality is fed into it, at least the same repeatability of 0.78 pixels is attainable. This is equivalent to 0.13 mm in the middle of the measurement line and to 0.09 mm at the edge.

The depth resolution of the flatness measurements was tested using accurate aluminium wave references with known heights of 0.6 mm, 1.5 mm, 3.0 mm and 5.0 mm. The phase shifts in the moiré signals were measured in the middles of two parallel lighting units of different depth sensitivity. The phase shifts as a function of the known height differences are presented in Fig. 33.
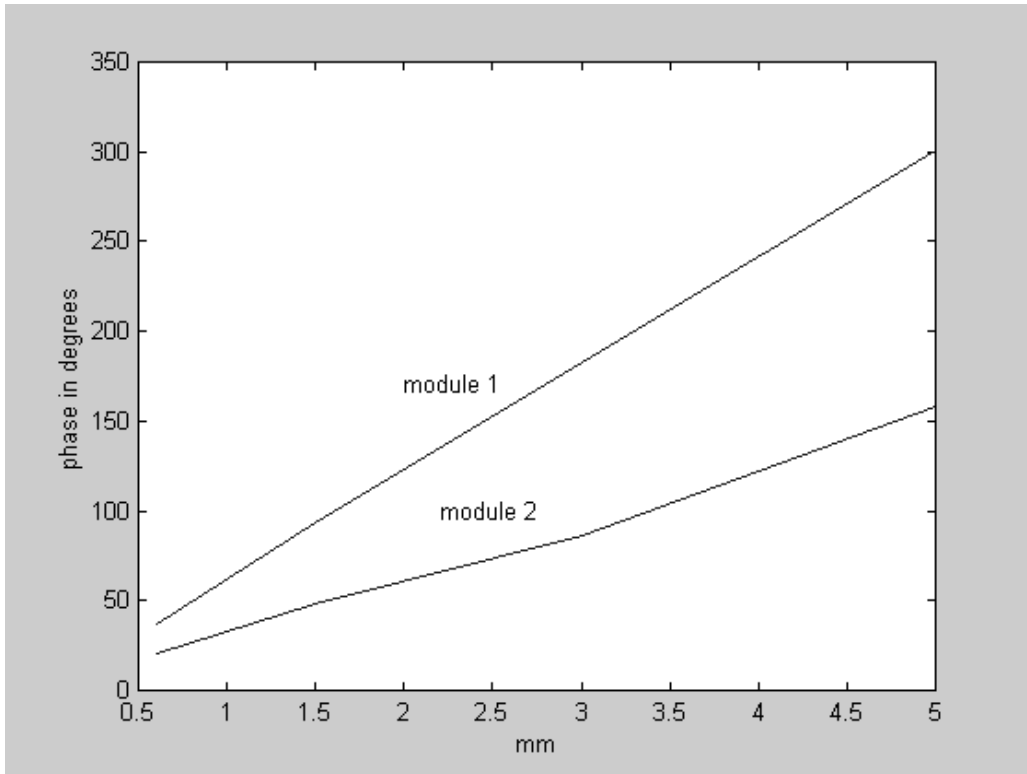
73

Figure 33. Phase shifts as a function of known height differences.

When the 0.6 mm reference was tested under the lighting unit with lowest sensitivity the fringe deformation was 3.5 pixels, which is equivalent to 21° (see Fig. 33). The depth resolution of the system is better than 0.6 mm. The deduced 4σ value for repeatability is 1.56 pixels, equivalent to a depth resolution of 0.27 mm.

5.2.2 Performance of the width measurement function

The repeatability and resolution of the system's width measurement function were evaluated in performance tests.

The locations of the static edges of an electrically galvanized steel plate were measured 90 times, giving a standard deviation for these measurements of 0.02 pixels, corresponding to 0.012 mm and indicating the amount of internal noise in the system. The maximum deviation was 0.1 pixels, which is equivalent to 0.06 mm in the prototype system. The internal noise of the system limits the maximum achievable resolution in width measurement.

The sample was moved transversely in 0.1 mm steps, equivalent to 0.17 pixels in the middle of the field of view and 0.14 pixels at the edge. An edge movement of 0.1 mm can be detected reliably and the resolution of the width measurement is better than 0.1 mm.

The repeatability of width measurements was tested with a sample from the pickling line and a sample of hot galvanized steel. The two edges of these samples had been machined to be parallel straight lines, and the widths of the samples were measured 30 times at one point on each. The repeatability was 2.88 pixels (2σ) for the pickled steel plate, corresponding to 1.73 mm, and 2.08 pixels (2σ) for the hot galvanized steel, corresponding to 1.25 mm. These results are not as good as could be expected in view of the above static edge resolution tests. The variations in sample positions and orientations in the measurement area evidently altered the intensity profiles of the edges. As plate or strip products have practically vertical, parallel edges, several successive edge locations could be averaged for the purposes of width measurement, or else a line fitting estimate could be used. This would improve the repeatability of width measurement.

The results suggest that it is feasible to measure the width of the steel plates or strips using the multipurpose flatness measurement system, but any variation in surface quality or the mechanical edge profile will tend to detract from the performance of optical width measurement.

5.2.3 Performance of the surface quality inspection function

As surface quality inspection has been a secondary task relative to the dimensional measurements, and as the image acquisition system is not specially designed for surface inspection, no performance evaluation was carried out regarding this aspect. Only the spatial resolution of the surface inspection function in the multipurpose flatness measurement system was evaluated using special test patterns, the results showing it to be 0.6 mm in the transverse direction and 0.9 mm in the longitudinal direction. These results are equal to the precalculated estimates. Longitudinal resolution depends on the line speed and the integration time of the camera.

6 DISCUSSION

The two types of moiré flatness measurement system described in Chapters 3 and 4 differ in both design and performance. The differences lie in the manner of moiré contour formation, as the same image processing algorithm is used in both, with only minor changes.

The feature that distinguishes most between these two systems is related to the moiré measurement principle. The system presented in Chapter 3 is based on optical projection moiré and can take advantage of optical leveraging over the large surface area, while that presented in Chapter 4 uses a grating projected onto a transverse measurement line and logical moiré for contour formation. When the latter system is used the plates are supposed to move on the production line, as stationary plates cannot be measured, whereas the first system provides an opportunity to inspect the plate both visually and numerically in a static situation within the measurement area.

There is no remarkable difference in depth resolution between these two systems, that of the optical projection moiré system having been shown to be better than 0.3 mm and that of the novel multipurpose system better than 0.6 mm. The optical projection moiré system offers in theory and practice better sensitivity if needed, by means of optical leveraging, but its sensitivity has been reduced on purpose by using bias fringes. This facilitates fringe interpretation and makes the measurements more robust in the face of environmental disturbances.

The performance of the systems may obviously differ in terms of the repeatability of flatness measurements, although they are not compared here under comparable production conditions. According to the performance evaluation the repeatability of flatness measurements is about 0.1 mm in both systems. Disturbances or shape deformations during measurement due to vibration of the moving plates are not likely to be so great in area-based measurements as in line-based ones. The effects of vibration on the measurements under production conditions are unknown with either, because there is a lack of information on the vibration of moving plates and their shape deformations. It is nevertheless obvious as far as optical flatness measurements are concerned that vibrations and shape deformations should be minimized at the measurement site.

Better quality moiré contours and more reliable image processing over a larger range of plate products can be obtained with the multipurpose flatness measurement system than with the optical projection moiré system, and even almost entirely specular surfaces can be measured. This is mainly achieved by better lighting and 100 % modulated binary gratings, and by eliminating the effects of surface anomalies on the moiré contours. One valuable feature of the multipurpose system is its capability for measuring 2D dimensions of the plates in addition to their flatness. The novel concept of the multipurpose flatness measurement system has given promising results in laboratory, but the system has not been tested and the results have

not been verified in a real factory environment. Negotiations are in progress for pilot installation and testing of the system.

Although the optical projection moiré system is now in continuous operation at the plate mill, there is still research and development work to be done on it. The depth resolution and the repeatability of the flatness measurements are adequate in plate areas where the fringes can be detected and are not broken, and the usability of the system has been reported by the staff at the mill to be excellent. The development work should now be focused on adaptation of the measurement system to dynamic variations in steel plate surfaces. There should not be plate areas without measurements and the decisions required for levelling should be made by the measurement system rather than the operator. The measurement conditions should be stabilized as much as possible by eliminating environmental disturbances. More powerful illumination would be needed to achieve better contrast in the moiré fringes and robustness with respect to stray light. High-power strobed flash lamps are worth considering as light sources. Strobe lighting gives better protection against both stray light and plate movements, but may disturb the work of the operators. The latest camera technology includes several trends and technical features which could be useful in an optical moiré measurement system. The sensitivity of camera detectors is improving and the amount of intelligence embedded in them is increasing, so that it is becoming easier to capture less noisy moiré images, and which can then be preprocessed inside the camera using filtering circuits or DSP processing units. The gain and offset values are currently adjusted for the whole image, but future cameras may include the property of adjusting the response of each individual pixel. This would allow for active optimal digitization of the moiré image.

Triangulation systems can be applied to flatness measurement. The sensitivity needed in the steel plate application could be achieved with triangulation by employing multiple laser sources and matrix cameras over the width of the measurement line. Current linescan cameras usually have a pixel resolution which is three or more times better than the horizontal or vertical resolution of matrix cameras. A triangulation system corresponding to the multipurpose flatness measurement prototype would therefore need three matrix cameras. Each projected line in the prototype is covered by more than two pixels and the one moiré fringe period is about 58 pixels. The behaviour of the many narrow projected lines on the surface of the plate would be averaged by the logical moiré to form one moiré fringe which would then be analysed by the image processing facility. Triangulation systems typically image one laser strip several pixels wide and analyse its centre of gravity in the image. The moiré flatness measurement system can be considered to be more robust in the face of both local geometrical and visual surface variations, and has the advantage of this averaging procedure when sub-millimetre level flatness measurements are to be made. The robustness is improved by the use of the background illumination and minimization the effects of surface anomalies on flatness measurements.

Triangulation systems can be regarded as a competitor or alternative solution to moiré topographical systems. Their principle is well known and the development of suitable light sources, lasers, LCD projectors, cameras etc. supports them just as well as moiré systems. If triangulation point sensors are mounted above the object, they can provide a continuous representation over the entire plate only if many sensors are installed side by side, and this is obviously an expensive solution. When large areas are to be measured, optical moiré offers greater sensitivity, through optical leveraging, and the spatial resolution of the matrix-type detector is not regarded as limiting the resolution of the flatness measurements.

7 SUMMARY

Steel manufacturers are showing an increasing interest in measuring the flatness of rolled steel plates, motivated by many aspects such as the use of quality standards, automation needs, process development and the increasing needs of customers, and they are looking for commercial flatness measurement systems applicable to measurement sites of many types in rolling and levelling processes. Companies developing measurement systems are now introducing commercial non-contact optical flatness measurement systems and the necessary technology is now available, as a consequence of long-term research work that has been going on since the 1980's.

The goal of this work was to investigate the applicability of moiré technology to the on-line measurement of the flatness of large steel plates. When the work was started in 1992, projection moiré technology was introduced as a promising alternative, but no fully automated systems for measuring the varying surface properties of large planar objects had been implemented for use in hostile industrial environments. This thesis describes the design and performance of an automated on-line moiré flatness measurement system for use with large steel plates and evaluates its performance under both laboratory and factory conditions. The objective for depth resolution, 0.3 mm, is shown to be achievable, and resolution can be improved if necessary by reducing the number of bias fringes. The system can withstand the environmental disturbances present in the plate mill. When designing future applications, special attention must be paid to stabilization of the measurement site and adaptation of the system to the varying surface properties of steel plates. Projection moiré topography is a feasible and competitive technique for measuring the flatness of steel plates. The first pilot system was installed at the Rautaruukki Steel mill at Raahe in 1995 and is now operating continuously. The system is called FM3500 and is commercially available from Spectra-Physics VisionTech Oy.

Experiences with the first pilot system and the different requirements at an other measurement site led to the invention of a novel multipurpose flatness measurement system, the design and performance of which are also described in this thesis. This system has many advantages over traditional projection moiré topography. It allows reliable flatness measurements to be performed on steel plates having great variations in surface properties, and its competitiveness and usability have been enhanced by adding 2D dimensional measurements such as edges, width, length etc. and even surface quality inspection to the same unit. Its robust optomechanical construction allows easy adaptation to measurement sites close to the plates, and can be implemented without tight tolerances. The performance of the system has been tested in the laboratory. Flatness measurements show a depth resolution better than 0.6 mm and excellent signal quality. 2D dimensional measurements are feasible and work best with plate products that do not have much variation in the optical properties of their edges. The multipurpose flatness measurement system provides opportunities for

surface inspection, but more work is needed on algorithm development and application-specific optimization.

REFERENCES

ABB 1997. ABB Stressometer Measuring Roll. Product information.

Air Gage Company 1992. CADEYES 3D inspection system. Product guide.

Arai, Y. & Kurata, T. 1988. Binarization of scanning moiré fringe pattern. Optics and Lasers in Engineering, Vol. 8, Nos 3 & 4, pp. 263 - 275. ISSN 0143-8166

ASTM designation: A 568/A 568M - 96. 1996. Standard specification for steel, sheet, carbon, and high-strength, low-alloy, hot-rolled and cold-rolled, general requirements. ASTM American Society for Testing and Materials, 1996. 22 p.

Asundi, A. 1993. Computer aided moiré methods. Optics and Lasers in Engineering, Vol. 18, No. 3, pp. 213 - 238. ISSN 0143-8166

Asundi, A., Sajan, M. R., Olson, G. & Walker, J. N. 1994. Digital moiré applications in automated inspection. Machine Vision Applications, Architectures, and Systems Integration III, Boston, USA, 31 October - 2 November 1994. SPIE, Vol. 2347, pp. 270 - 275. ISBN 0-8194-1682-7

Asundi, A. & Sajan, M. R. 1995. Peripheral inspection of objects. Optics and Lasers in Engineering, Vol. 22, No. 3, pp. 227 - 240. ISSN 0143-8166

Bahners, T., Ringens, W. & Schollmeyer, E. 1994. On-line inspection of textile geometries. Laser Dimensional Metrology: Recent Advances for Industrial Application, Brighton, UK, 5 - 7 October 1993. SPIE, Vol. 2088, pp. 97 - 103. ISBN 0-8194-1359-3

Besl, P. J. 1988. Active optical range imaging sensors. Machine Vision and Applications, Vol. 1, No. 2, pp. 127 - 152. ISSN 0932-8092

Bieman, L. H. & Michniewicz, M. A. 1994. Large angle incoherent structured light projector. Imaging and Illumination for Metrology and Inspection, Boston, USA, 31 October - 4 November 1994. SPIE, Vol. 2348, pp. 165 - 169. ISBN 0-8194-1683-5

Blatt, J. H., Hooker, J. A., Belfatto, R. V. & Young, E. 1990. 3-D inspection of large objects by moiré profilometry. Southcon/90 Conference Record, Orlando, USA, 20 - 22 March 1990. Piscataway (NJ): IEEE. Pp. 96 - 100.

Blatt, J. H., Cahall, S. C. & Hooker, J. A. 1992 a. Variable resolution video moiré error map system for inspection of continuously manufactured objects. Industrial Applications of Optical Inspection, Metrology, and Sensing, Boston, USA, 19 - 20 November 1992. SPIE, Vol. 1821, pp. 296 - 303. ISBN 0-8194-1022-5

Blatt, J. H., Hooker, J. & Caimi, F. M. 1992 b. Adaptation of video moiré techniques to undersea mapping and surface shape deformation. Optics and Lasers in Engineering, Vol. 16, Nos 4 & 5, pp. 265 - 278. ISSN 0143-8166

Boehnlein, A. J. & Harding, K. G. 1989. Field shift moiré, A new technique for absolute range measurement. Fringe Pattern Analysis, San Diego, USA, 8 - 9 August 1989. SPIE, Vol. 1163, pp. 2 - 13. ISBN 0-8194-0199-4

Boehnlein, A. J. & Harding, K. G. 1986. Adaptation of a parallel architecture computer to phase shifted moiré interferometry. Optics, Illumination, and Image Sensing for Machine Vision, Cambridge, USA, 30 - 31 October 1986. SPIE, Vol. 728, pp. 183 - 194. ISBN 0-89252-763-3

Broner Group Ltd. 1991. Optiflat XAM. Technical Summary.

Cardenas-Garcia, J. F., Zheng, S. & Shen, F. Z. 1994. Implementation and use of an automated projection moiré experimental set-up. Optics and Lasers in Engineering, Vol. 21, Nos 1& 2, pp. 77 - 98. ISSN 0143-8166

Chiang, F. 1979. Moiré methods of strain analysis. Experimental Mechanics, Vol. 19, No. 8, pp. 290 - 308. ISSN 0014-4851

Cielo, P. 1988. Optical Techniques for Industrial Inspection. San Diego, USA: Academic Press Inc. 606 p. ISBN 0-12-174655-0

Clarke, T. A., Robson, S. & Chen, J. 1993. A comparison of three methods for the 3-D measurement of turbine blades. Measurement Technology and Intelligent Instruments, Wuhan, China, 29 October - 5 November 1993. SPIE, Vol. 2101, pp. 1 - 12. ISBN 0-8194-1384-4

Dirckx, J. J. J. & Decraemer, W. F., 1990. Automated 3-D surface shape measurement based on phase-shift moiré. Optics in Complex Systems, Garmisch-Partenkirchen, West Germany, 5 - 10 August 1990. SPIE, Vol. 1319, pp. 348 - 349. ISBN 0-8194-0380-6

Dolan-Jenner Industries 1993. TDC, Three dimensional camera. Product information.

Dykes, B. C. 1970. Analysis of displacements in large plates by the grid-shadow moiré technique. Experimental Stress Analysis and its Influence on Design, Cambridge, England, 6 - 10 April 1970. London: Institution of the Mechanical Engineers; Joint British Committee for Stress Analysis. Pp. 122 - 131.

Electro-Optical Information Systems 1996. EOIS mini-moire sensor. Product information.

Gåsvik, K. J., Hovde, T. & Vadseth, T. 1989. Moiré technique in 3-D machine vision. Optics and Lasers in Engineering, Vol. 10, Nos 3 & 4, pp. 241 - 249. ISSN 0143-8166

Grant, I., Stewart, N. & Padilla-Perez, I. A. 1990. Topographical measurements of water waves using a projection moiré method. Applied Optics, Vol. 29, No. 28, pp. 3981 - 3983. ISSN 0003-6935

Harding, K. G. 1994. Optical moiré leveraging analysis. Imaging and Illumination for Metrology and Inspection, Boston, USA, 31 October - 4 November 1994. SPIE, Vol. 2348, pp. 181 - 188. ISBN 0-8194-1683-5

Harding, K. G. 1996. Theory and operation of moire contouring. Industrial Technology Institute, Electro-Optics Engineering, Machine Vision & Laser Gaging Technical Papers. [Cited 10/07/96.] 6 p. Available from Internet: http://www.iti.org/eoe/papers/mtheory.txt.

Harding, K. G. & Sieczka, E. J. 1993. 3D moiré methods applied to shape recognition. In: Proc. International Robots and Vision Automation Conference, Detroit, 5 - 8 April 1993. Ann Arbor: Robotic Industries Association. Pp. 13 - 22.

Harding, K. G., Kaltenbacher, E. & Bieman, L. H. 1990. Single lens contouring method. Optics, Illumination, and Image Sensing for Machine Vision V, SPIE, Vol. 1385, pp. 246 - 255. ISBN 0-8194-0452-7

Harding, K. G., Coletta, M. P. & VanDommelen, C. H. 1988. Color encoded moiré contouring. Optics, Illumination and Image sensing for Machine Vision III, Cambridge, USA, 8 - 9 November 1988. SPIE, Vol. 1005, pp. 169 - 178.

Hauer, M. W. & Harding, K. G. 1990. Design of a moiré interferometer for surface defect inspection. Robotics and Vision Conference, Detroit, June 1990. Pp. 3 - 15.

Heaven, M. E. 1988. Ideal flatness sensor requirements. Hot Strip Mill Profile and Flatness Seminar, Pittsburgh, Pennsylvania, 2 - 3 November 1988. Pittsburgh: AISE. Pp. 1 - 16.

Hoy, D. E. P. 1992. Color digital imaging system for bicolor moiré analysis. Experimental Techniques, Vol. 16, No. 3, pp. 25 - 27. ISSN 0732-8818

Hu, C.-H. & Qin, Y.-W. 1997. Digital color encoding and its application to the moiré technique. Applied Optics, Vol. 36, No. 16, pp. 3682 - 3685. ISSN 0003-6935

Ibrahim, M. D. & Takasaki, H. 1985. Two-frequency moiré topography. Japanese Journal of Applied Physics, Vol. 24, No. 9, pp. 1181 - 1182.

Kaczér, J. & Kroupa, F. 1952. The determination of strain by mechanical interference. Czechoslovak Journal of Physics, Vol. 1, No. 2, pp. 80 - 85.

Kitamura, K., Kawashima, K. & Soga, H. 1981. An application of moiré topography to 3-dimensional shape measurement of hot steel. Control Science and Technology for the Progress of Society: preprints of the 8th triennial world congress of International Federation of Automatic Control (IFAC), Kyoto, 24 - 28 August 1981. Kyoto: IFAC. Pp. 88 - 93. ISBN 0-08-027580-x

Kozlowski, J. & Serra, G. 1997. New modified phase locked loop method for fringe pattern demodulation. Optical Engineering, Vol. 36, No. 7, pp. 2025 - 2030. ISSN 0091-3286

Kujawinska, M. 1993. The architecture of a multipurpose fringe pattern analysis system. Optics and Lasers in Engineering, Vol. 19, Nos 4 & 5, pp. 261 - 268. ISSN 0143-8166

Kujawinska, M. & Patorski, K. 1993. New trends in optical methods for experimental mechanics. Part I: moiré and grating projection techniques for shape and deformation measurement. Journal of Theoretical and Applied Mechanics, Vol. 3, No. 31, pp. 539 - 561. ISSN 0079-3701

Lim, J. S. & Chung, M. S. 1988. Moiré topography with color gratings. Applied Optics, Vol. 27, No. 13, pp. 2649 - 2650. ISSN 0003-6935

LIMAB 1996. LMS Shapemeter. Product information.

Lohmann, A. W. & Po-Shiang, L. 1980. Computer generated moiré. Optics Communications, Vol. 34, No. 2, pp. 167 - 170. ISSN 0030-4018

Mairy, B., Balthasart, P. & Lückers J. 1988. Review of the five last applications of the ROMETER flatness gage and perspectives. Hot Strip Mill Profile and Flatness Seminar, Pittsburgh, Pennsylvania, 2 - 3 November 1988. Pittsburgh: AISE. Pp. 1 - 11.

Matsuo, J., Matsumi, T. & Kitamura, K. 1990. Plate flatness meter based on moiré fringes. IAPR Workshop on Machine Vision Applications, Tokyo, 28 - 30 November 1990. Tokyo: IAPR. Pp. 97 - 100.

Meadows, D. M., Johnson, W. O. & Allen, T. B. 1970. Generation of surface contours by moiré patterns. Applied Optics, Vol. 9, No. 4, pp. 942 - 947. ISSN 0003-6935

Mills, H., Burton, D. R. & Lalor, M. J. 1995. Applying backpropagation neural networks to fringe analysis. Optics and Lasers in Engineering, Vol. 23, No. 5, pp. 331-341. ISSN 0143-8166

Mousley, R. F. 1985. A shadow moiré technique for the measurement of damage in composites. Composite Structures, Vol. 4, No. 3, pp. 231 - 244. ISSN 0263-8223

Mulot, M. 1925. Application of the moiré to the study of mica deformations. Review D'Optique, Vol. 4, May, pp. 252 - 259.

Murakami, K., Murakami, Y. & Seino, T. 1982. On the setting of the light source for the grid illuminating type moiré method. Annals of the CIRP, Vol. 31, No. 1, pp. 405 - 407. ISSN 0007-8506

Murakami, K., Murakami, Y. & Seino, T. 1985. A procedure for setting up exactly the camera for the grid illuminating type moiré method. Bull. Japan Society of Prec. Eng., Vol. 19, No. 4, pp. 249 - 253. ISBN 0582-4206

Murakami, K., Murakami, Y. & Seino, T. 1989. Problems with the grid-illuminating-type moiré method and procedures for solving them (theory). JSME International Journal, Vol. 32, No. 3, pp. 374 - 377. ISSN 0913-185x

Nordbryhn, A. 1983. Moiré topography using a charge coupled device television camera. Industrial Applications of Laser Technology, Geneva, Switzerland, 19 - 22 April 1983. SPIE, Vol. 398, pp. 208 - 213.

Nurre, J. H. & Hall, E. L. 1992. Encoded moiré inspection based on the computer solid model. IEEE Transactions on Pattern Analysis and Machine Intelligence, Vol. 14, No. 12, pp. 1214 - 1218. ISSN 0162-8828

Paakkari, J. 1993. Method for evaluating the performance of range imaging devices. Oulu, Finland: University of Oulu. Licenciate Thesis. 64 p.

Paakkari, J. & Moring, I. 1993. Method for evaluating the performance of range imaging devices. Industrial Applications of Optical Inspection, Metrology, and Sensing, Boston, USA, 19 - 20 November 1992. SPIE, Vol. 1821, pp. 350 - 356. ISBN 0-8194-1022-5

Pat. US. 5,307,152. 1994. Moiré inspection system. Industrial Technology Institute. (Boehnlein, A. & Harding, K.) Appl. No. 954,761, 29.9.1992. 26.4.1994. 13 p.

Pat. US. 5,488,478. 1996. Method and apparatus for measuring the shape of a surface of an object. British Steel PLC (Bullock, J. & Williams, N.) Appl. No. 290,811, 15.2.1993. 30.1.1996. 11 p.

Patorski, K. & Kujawinska, M. 1993. Handbook of the moiré fringe technique. The Netherlands: Elsevier Science Publishers. 431 p. ISBN 0-444-88823-3

Pekelsky, J. R. & van Wijk, M. C. 1989. Moiré topography: Systems and applications. In: Non-Topographic Photogrammetry. 2nd ed. Karara, H. M. (ed.). Falls Church, VA: American Society for Photogrammetry and Remote Sensing. Pp. 231 - 263. ISBN 0-944426-23-9

Perry, K. E. & McKelvie J. 1993. A comparison of phase shifting and fourier methods in the analysis of discontinuous fringe patterns. Optics and Lasers in Engineering, Vol. 19, Nos 4 & 5, pp. 269 - 284. ISSN 0143-8166

Rahkola, K. 1997. New multipurpose 3D-measuring technics. Machine Vision News. Helsinki: The Vision Club of Finland, Vol. 2, p. 11.

Reid, G. T., Rixon, R. C. & Stewart, H. 1987. Moiré topography with large contour intervals. Photomechanics and Speckle Metrology, San Diego, USA, 17 - 20 August 1987. SPIE, Vol. 814, pp. 307 - 313.

Rodriguez-Vera, R. 1994. Three-dimensional gauging by electronic moiré contouring. Revista Mexicana de Fisica, Vol. 40, No. 3, pp. 447 - 458. ISSN 0035-001x

Schmit, J. 1996. Spatial phase measurement techniques in modified grating interferometry (strain, error reduction). University of Arizona. Ph.D. Thesis. 192 p.

Sciammarella, C. A.1982. The moiré method - A review. Experimental Mechanics, Vol. 22, No. 11, pp. 418 - 433. ISSN 0014-4851

Servin, M., Rodriguez-Vera, R. & Malacara, D. 1995. Noisy fringe pattern demodulation by an iterative phase locked loop. Optics and Lasers in Engineering, Vol. 23, No. 5, pp. 355-365. ISSN 0143-8166

SFS-EN 10 029. 1991. Hot rolled steel plates 3 mm thick or above - Tolerances on dimensions, shape and mass. Helsinki, Finland: Finnish Standards Association. 12 p.

Sieczka, E. 1992. Feasibility of moiré interferometry for flatness checking of steel plates. Industrial Applications of Optical Inspection, Metrology, and Sensing, Boston, USA, 19 - 20 November 1992. SPIE, Vol. 1821, pp. 428 - 438. ISBN 0-8194-1022-5

Sieczka, E. J., Paakkari, J. & Moring, I. 1993. Flatness checking of metal surfaces using moire interferometry. Automaatiopäivät, Helsinki, Finland, 11 - 13 May 1993. Helsinki: Finnish Society of Automation. Pp. 358 - 362. ISBN 951-96042-5-1

Sough, D. 1993. Beyond fringe analysis. Interferometry, San Diego, USA, 12 - 13 July 1993. SPIE, Vol. 2003, pp. 208 - 223. ISBN 0-8194-1252

Spectra-Physics VisionTech Oy 1996. FM3500, Flatness measurement system. Product information.

Steinbichler, H. 1990. New options of holographic and similar measurement techniques applied to car construction. Practical holography IV, Los Angeles, USA, 18 - 19 January 1990. SPIE, Vol. 1212, pp. 241 - 256.

Suzuki, M. & Kanaya, M. 1988. Applications of moiré topography measurement methods in industry. Optics and Lasers in Engineering, Vol. 8, Nos 3 & 4, pp. 171 - 188. ISSN 0143-8166

Suzuki, M. & Suzuki, K. 1982. Moiré topography using developed recording methods. Optics and lasers in Engineering, Vol. 3, No. 1, pp. 59 - 64. ISSN 0143-8166

Tabatabai, A. J. & Mitchell, R. 1984. Edge location to subpixel values in digital imagery. IEEE Transactions on Patterns Analysis and Machine Intelligence, Vol. PAMI-6, No. 2, pp. 188 - 201. ISSN 0162-8828

Takasaki, H. 1970. Moiré topography. Applied Optics, Vol. 9, No. 6, pp. 1467 - 1472. ISSN 0003-6935

Takeda, M. 1982. Fringe formula for projection type moiré topography. Optics and Lasers in Engineering, Vol. 3, No. 1, pp. 45 - 52. ISSN 0143-8166

Theocaris, P. S. 1964. Moiré method in plates. In: Proc. of the IASS Symposium, Non-Classical Shell Problems, Warsaw 1964. Amsterdam: North-Holland. Pp. 877 - 889.

Tsuno, T. & Nakamura, Y. 1978. Accuracy of the measurement in moiré topography (continued report). Annual Report of the Engineering Research Institute Faculty of Engineering, University of Tokyo, Vol. 37, pp. 153 - 157. ISSN 0374-2482

Varman, P. O. 1984. A moiré system for producing numerical data of the profile of a turbine blade using a computer and video store. Optics and Lasers in Engineering, Vol. 5, No. 1, pp. 41 - 58. ISSN 0143-8166

Weller, R. & Shephard, B. M. 1948. Displacement measurement by mechanical interferometry. Proceedings of the SESA, Vol. 6, No. 1, pp. 35 - 38.

Vinarub, E. & Kapoor, N. 1992. Reverse engineering "A new definition for the nineties". In: Proc. of the IEEE 1992 National aerospace and electronics conference, NAECON 1992, Dayton, USA 18 - 22 May 1992. New York: IEEE. Pp. 1213 - 1219. ISBN 0-7803-0652-x

Warsaw University of Technology, Optical engineering division. Projection - moire system for surface form measurement. Laboratory information.

Wegdam, A. M. F., Podzimek, O. & Hallie, H. 1992. Projection moiré system simulation. Applied Optics, Vol. 31, No. 19, pp. 3755 - 3758. ISSN 0003-6935

Wiese, D. R., Ohlson, L., Hammerstrom, H. & Broman, H. 1982. Continuous on-line measurement of hot strip flatness. Iron and Steel Engineer, Vol. 59, No. 3, pp. 49 - 52.

Xie, X., Atkinson, J. T., Lalor, M. J. & Burton, R. D. 1996. Three-map absolute moiré contouring. Applied Optics, Vol. 35, No. 35, pp. 6990 - 6995. ISSN 0003-6935

Yatagai, T. & Idesawa, M. 1981. Automatic measurement of 3-D shapes using scanning moiré method. In: Conference on Optics in four Dimensions, Ensenada, Mexico, 4 - 8 August 1980. Machado, M. A. & Narducci, L. M. (eds.). New York: American Institute of Physics (AIP). AIP conference proceedings, Optical Science and Engineering, series 1, pp. 579 - 584. ISBN 0-88318-164-9